CONF-8309208--3

UCRL--89700

DE86 000738

Broad-band Soft X-ray Diagnostic Instruments at the LLNL Novette Laser Facility

K. G. Tirsell, P. H. Y. Lee,
D. G. Nilson, and H. Medecki

This paper was prepared for submittal to
the 16th European Conference on
Laser Interaction with Matter
Imperial College, London

September 15, 1983

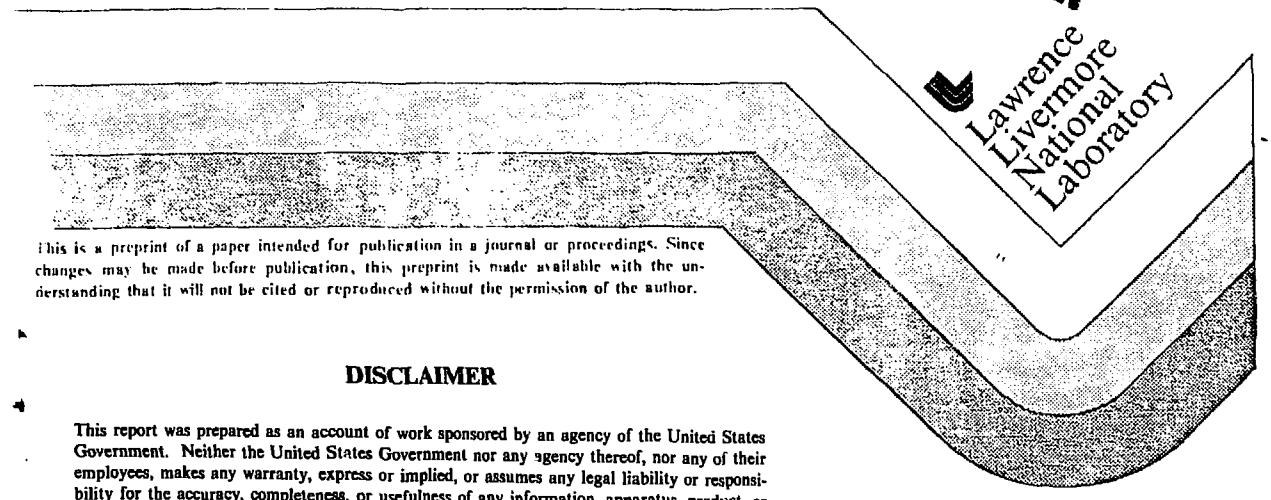

DISCLAIMER

Broad-band Soft X-ray Diagnostic Instruments at the LLNL Novette Laser Facility*

K. G. Tirsell, P. H. Y. Lee, D. G. Nilson, and H. Medecki

Lawrence Livermore National Laboratory
P.O. Box 5508
Livermore, California 94550

Abstract

Complementary broad-band instruments have been developed to measure time dependent, absolute soft x-ray spectra at the Lawrence Livermore National Laboratory (LLNL) Nd glass laser irradiation facilities. Absolute flux measurements of x rays emitted from laser-produced plasmas are important for understanding laser absorption and energy transport. For a number of years, arrays of filtered x-ray diodes, some with grazing incidence mirrors, have been used as primary instruments because they are reliable and can be accurately calibrated. We will describe two new 10-channel XRD systems that have been installed at the LLNL Novette facility for use in the 0.15- to 1.5- keV range. Since XRD channel time response is limited by available oscilloscope performance to 120 ps, a soft x-ray streak camera has been developed for better time resolution (20 ps) and greater dynamic range ($\sim 10^3$) in the same x-ray energy region. Using suitable filters, grazing incidence mirrors, and a gold or cesium-iodide transmission cathode, this streak camera instrument has been installed at Novette to provide one broad and four relatively narrow channels. It can also be used in a single channel, spatially discriminating mode by means of pinhole imaging. The complementary nature of these instruments has been enhanced by locating them in close proximity and matching their channel energy responses. As an example of the use of these instruments, we present results from Novette 2ω(0.53 μm) gold disk irradiations at 1 ns and 10^{14} to 10^{15} W/cm^2.

*Work performed under the auspices of the U.S. Department of Energy by Lawrence Livermore National Laboratory under Contract W-7405-Eng-48.

I. Introduction

Measurements of x-ray emission from irradiated targets are of particular importance to the Lawrence Livermore National Laboratory's Fusion Experiments Program. A number of different x-ray diagnostic instruments have therefore been designed and are in use at the LLNL Novette 2ω (0.53 μm) laser facility.[1] In this article, we describe broad-band instruments that have been developed to measure soft x-ray spectra consisting of two very similar x-ray diode (XRD) based systems, locally called Dante spectrometers, and a spatially discriminating instrument, called the SDSS, that utilizes an LLNL soft x-ray streak camera.

The Dante spectrometers are designed to measure absolute, time dependent, x-ray spectra in the energy range from 0.15 to 1.5 keV using ten K-or L-edge filtered channels with relatively broad, ~ 200 eV, energy resolution.[2] Three of the lowest energy Dante channels employ grazing incidence mirrors for better energy discrimination.

The SDSS instrument, also featuring broad-band, filtered channels and grazing incidence mirrors, was developed to take advantage of the 20-ps time resolution capability and great dynamic range (10^3) of the LLNL streak camera.[3] Five SDSS channels have been designed for Novette, although in its spatially discriminating mode obtained by using an accurately aligned pinhole, the instrument is restricted to one channel.

Our present operational plan is to rely on the SDSS for superior time resolution and spatial discrimination and on the Dante spectrometers for absolute x-ray spectral measurements and eventually to closely correlate the data obtained with these instruments.

In section II we describe the experimental arrangement of broad-band x-ray diagnostic instruments at the Novette facility. The time responses of the Dante and SDSS instruments are discussed briefly in section III. The channel energy responses of these instruments are presented in section

V after a discussion in section IV of the Dante spectrometer energy response calibration techniques. In section VI we present, as an example, some experimental results from a Novette 0.53 μm gold disk irradiation at 1 ns and 3 x 10^{14} w/cm^2.

II. Novette Experimental Arrangement

Figure 1 shows the target chamber and several diagnostic instruments at the LLNL Novette laser irradiation facility. The instruments used for soft x-ray measurements are shown mounted roughly orthogonal to the axes of the two Novette Nd glass laser beam lines. The two 10-channel Dante XRD arrays are horizontally positioned on opposite sides of the chamber. The filter- fluorescer spectrometer used for x-ray measurements above five keV is shown near the Dante-H spectrometer.

To facilitate the correlation of results, the SOSS instrument has been mounted as close as possible, being 18^o directly above the Dante-H instrument. Not shown in Fig. 1 is an x-ray transmission grating coupled to a streak camera designed to record continuous soft x-ray spectra with very good temporal resolution.[4] This instrument is located in close proximity to the Dante-A system to enhance our correlations of results. Also prominently shown mounted on the Novette target chamber are four target alignment viewers and several energy balance modules.

Figure 2 shows a schematic of the Dante-H XRD spectrometer installed at Novette. Except for several significant improvements such as more rigid stainless steel flight tubes, these spectrometers are similar to the instruments used at the Shiva facility that have been described previously.[2] The nearly identical Novette Dante systems (H and A) each consist of two sets of five filtered XRDs located on a flight tube that is evacuated to 10^{-6} Torr using a vertically mounted cryostat pump. The flight tube is supported on a new front pivot assembly so that its axis can be easily and accurately aligned with the aid of a rear mounted, centerline laser. Three grazing incidence mirrors are located on the back array of each Novette Dante spectrometer. These self-contained mirror

cassettes, designed by Lockheed, have been recently recalibrated at LLNL.[5] One of our most significant improvements has been the development of one-micron thick boron filters at LLNL and the recalibration of our carbon mirrors that has enabled us to use a very good channel with a 185-eV filter edge.

A typical mirror Dante channel is shown in Fig. 3 consisting of a tantalum beam defining collimator, a thin parylene pre-filter, from one to three vanadium filters in a removable housing, a mirror cassette, and an electrically isolated, windowless, aluminum XRD. The 82% transmitting nickel mesh anode is biased to +5 kV. The removable, diamond-turned, aluminum cathode is tapered to match a 50-ohm feedthrough coupled to an oscilloscope by means of a good quality air-heliax signal cable.

For approximately one-half of its lifetime to date, the Novette SDSS instrument has been used with spatial discrimination provided by a 100-micron diameter pinhole, providing a 10X magnification. This pinhole decreases the x-ray flux on the streak camera entrance slit to such an extent that our most sensitive cathode material, cesium-iodide, is required. In this case, we select the most sensitive carbon filtered channel that invariably yields the greatest film exposure. Due mainly to severe pinhole alignment tolerances, our proposal to record two separate channels, each with its own pinhole and requiring half the available streak camera cathode entrance slit length, has not yet been implemented.

Figure 4 shows a schematic of the SDSS in its other mode of operation without spatial discrimination. Other versions of the instrument have been described previously.[3] This SDSS version features a streak camera with a gold transmission cathode sensitive to x rays >100 eV and a set of thin filters providing five different channels. Each channel has an appropriate grazing incidence mirror designed to greatly decrease x-ray contributions beyond its filter cut-off energy. The Novette SDSS version also features a thin (800 Å) aluminum filtered channel designed for significantly greater sensitivity and very broad coverage in the energy region below ~1.5 keV.

III. Time Response

One of the main reasons for developing the 20 ps SDSS spectrometer is that the Dante channel time response is limited by available oscilloscope performance to response times (FWHM) of approximately 120 ps. Fig. 5 summarizes the time response characteristics of these instruments. For ease of operation the Novette Dante systems are presently configured to use amplified and direct-access Tektronics 7912 transient digitizers with 730 and 335 ps FWHM times respectively. To upgrade the performance, we plan to multiplex eight Dante detectors into a system of four Thomson TSN-660 high performance oscilloscopes. This program depends critically on the development of a streamlined, computer based, polaroid film digitizing facility.

The Novette SDSS instrument has been adjusted to record data out to four ns. In this mode, the system resolution increases to $\sim$ 60 ps, which is certainly adequate to measure detailed time histories of 1-ns Novette experiments.

IV. Calibration of Dante Channel Responses

In this section, we discuss Dante channel energy response calibrations, since we are relying on the Dante spectrometers for absolute spectral measurements. We intend to calibrate the SDSS channels on-line at Novette by directly comparing results with those from corresponding Dante-H channels.

As has been discussed previously,[2] the response of a Dante channel is determined by calibrating each of its components separately. Nearly all of our energy response measurements have been made using the facilities of the LLNL Calibration and Standards Laboratory. Figure 6 shows examples of filter transmission results obtained at the LLNL Ionac, our proton induced, monoenergetic sub-keV x-ray generator. The filter data analysis has been expedited with routines recently developed using

the Fusion Experiments Analysis Facilities' VAX computer and its ORACLE data-base management system.[6] The process code uses compound or elemental cross sections to generate a least-squares theoretical fit to the appropriate transmission data with areal density of each constituent as a fitted parameter. Compound specifications, transmission data, and calculated areal densities are all stored using the ORACLE data-base management system. The results shown for the parylene-N filter are typical of the pre-filters used on almost every Dante channel. The excellent fit suggests that both the specified 86% mesh transmission value and our parylene material specifications are reasonable. The results shown for Formvar[7] are good for all points except those on either side of the oxygen K-edge due most probably to the slight spread of IONAC source L-lines. For cobalt and copper, best fits are obtained by specifying both the element and its oxide. Note that in each case a reasonable value for the oxide thickness was determined by the code.

Fig. 7 shows typical measured XRD quantum efficiencies which have been discussed previously.[8] Data below one keV were obtained at the IONAC and above one keV from the LEXF.[9] The smooth curves are normalized values of $E\mu(E)$, where E is the x-ray energy and $\mu(E)$ is the photo-ionization cross section obtained from Henke, et al.[10] As has been noted by Henke, this simple model works reasonably well except at cathode material absorption edges.[11] The results for Al suggest that a better fit for this extensively used cathode material lies between Al and Al_2O_3. For both Cr and Ni cathodes, adding a small fraction of the respective oxide tends to produce better fits. For gold, the only cathode material not used in Novette systems, the $E\mu(E)$ model gives a better representation of the quantum efficiency shape, even across the main gold M-edges. In generating detector sensitivity curves, we use the $E\mu(E)$ model only as a guide for interpolating between calibration values.

The Dante grazing incidence mirrors that we are using at Novette were calibrated at the IONAC.[5] Fig. 8 shows the IONAC x-ray reflectivity data for two carbon mirrors at 5^0 used for the boron-filtered channels. The best-fit theoretical curve for both mirrors was obtained by scaling

the reflectivity values calculated using the REFLECT2 computer code[12] by a factor of 0.86. The measured reflectivity values for the two beryllium mirrors at 3.4°, shown in Fig. 9, are reasonable well fit with the REFLECT2 code by assuming a weighted composition of Be and beryllium oxide. Note however that this calculation is not rigorous because the real material is in two layers rather than being uniformly distributed. A second calculational problem is that REFLECT2 does not yet take into account the higher order effects that are very significant at and near material absorption edges.[13] The experimental data for the carbon mirror at 2.4°, shown in Fig. 10, are fit reasonably well in the important x-ray energy region below the vanadium L-filter edge using REFLECT2 and an 82% scale factor. Experimental values are comparatively high near the carbon K-edge as expected[13] and high at the 704eV, IONAC, Fe-L source line for reasons yet to be explained. Work on the mirror calibration data analysis is still in progress.

V. Channel Response vs Energy

In this section, we present and compare channel energy responses of the Novette Dante and SDSS instruments. Three Dante channels have counterparts in the SDSS spectrometer. Figs. 11, 12, and 13 respectively show our Dante response calibration results for the channel components along with the total responses that have been derived. For example, the filter transmission curve for the parylene channel shown in Fig. 11 was obtained from data for two parylene filters of 3.5-μm measured thickness. Note that two out of three of the Dante channels have grazing incidence mirrors.

The absolutely calibrated, channel energy responses of the ten Novette Dante-H channels are summarized in Figs. 14 and 15. Compared to the Shiva instruments,[2] significant improvements in coverage and energy resolution have been made below 600eV through the use of thicker filters and grazing incidence mirrors as well as to the addition of the boron channel.

Figure 16 shows normalized channel responses for the Novette SDSS instrument. Note that the two aluminum-filtered channels are relatively broad and that the thin Al channel is much more sensitive than any of the others. The responses of the three narrow SDSS channels below 800 eV are compared directly with their corresponding Dante channels in Fig. 17. Two instrumental changes are required to obtain the very good shape agreement shown for all three cases. A new fused-silica mirror at 3^{o} needs to be installed on the SDSS carbon channel and three rather than two existing filters need to be used in the Dante vanadium channel. Note that cobalt channel comparisons are generally not strongly affected by contributions beyond the Dante filter edge. This is because most of the spectra that we measure tend to decrease rapidly above 1 keV.

VI. Example of Measurements - A Novette Gold Disk Irradiation

As an example of our results, we have chosen a Novette gold disk irradiation with the experimental conditions summarized in Fig. 18. In this geometry, the SDSS instrument is in its spatially discriminating mode with an edge-on view to observe ∿200 eV x-ray emission from the ablating surface of a disk target irradiated from one side. The Dante-H spectrometer has a view of the disk similar to that of the SDSS. The slight angular variations of the Dante channels and the rapid change of the spectrum with angle near the edge make it difficult to unfold a reasonable Dante-H spectrum. Instead we will present spectral results obtained with the Dante-A spectrometer that views the disk surface at an angle β of 75^{o} with respect to the disk normal. (Internal instrumental corrections made assuming a cos β emission dependence are less than 20% at this angle.)

Figure 19 shows the SDSS streak record for this shot with the laser beam incident from the right. The spatial axis is horizontal and the time axis is vertical. An isodensity plot of this photo-densitometered streak record is shown in Fig. 20, with the time scale in nanoseconds and length scale in microns. Figs. 21 to 25 show corresponding lineouts at spatial positions 560, 650 , 710 , 780 and 930 μm respectively, yielding the

temporal profiles of the 200 eV emission at these locations. The maximum emission region is located between 560 and 600 μm. This is also the position where the x-ray emission occurs the earliest, indicating that this is the front surface where the laser pulse first impinged on the disk. One observes that the peak emission time occurs later as the sampled spatial position is moved out further away from the original front surface position. Using a time-of-flight method, we estimate from these figures a value for the velocity of $(3.8\pm0.5)\times10^7$ cm/s for the speed with which the 200 eV emission region is moving.

Figure 26 shows representative Dante-A oscilloscope signals that have been aligned on their leading edges and overlayed to show the time dependence of the spatially integrated, spectral emission. A slightly more accurate analysis can be made by deconvoluting narrower signals thus taking into account the impulse responses of the respective channels. The conclusions, however, are the same. Above 500 eV, the x-ray emission FWHMs are not significantly greater than the 1-ns laser pulse time width, and there is a very gradual decrease in emission width with increasing x-ray energy. The two lowest energy channels at 160 eV and 220 eV have corresponding pulse shapes that are slightly greater than the laser pulse.

These detector signals were integrated to determine the detector charge- per-channel over the duration of the prompt x-ray pulse. The results, along with the system channel energy responses of Fig. 27, were used in a new version of UNSPEC, the LLNL spectral unfolding code,[14] to obtain the spectrum shown in Fig. 28. The spectral points are plotted to show the deviations of the individual channels from the smoothed spectrum that best fits all the data. The channel-by-channel integrals of the response-times-best-fit spectrum that have been plotted in Fig. 27 give an indication of the good coverage and data quality that can be obtained with this broad-band instrument. Note that each of the spectral points is plotted at the 50% value of its respective response-times-spectrum integral curve.

Note that the measured spectrum rises to a peak at ~700eV in the energy region dominated by gold N-line generation. The spectrum drops

rapidly above one keV. Note also that the spectral emission from the disk is relatively low below 500 eV compared to 2ω-gold disk results obtained at this intensity at the LLNL Argus Laser Facility[15] using much less total laser energy (25J) and much smaller spot sizes (180-μm diam).

Figure Captions

1. Diagnostic instruments on the LLNL Novette target chamber.

2. Ten-channel array of filtered x-ray diodes at the Novette laser facility.

3. Typical filtered-XRD channel with a grazing incidence mirror.

4. A schematic of the multichannel, filtered-mirrored, soft x-ray streak camera, SDSS, at the Novette laser facility.

5. Measured impulse time responses of four LLNL XRD detector-signal cable-oscilloscope systems[2] compared to that of the SDSS. System A: The LLNL 50-ps detector into a TSN-660 oscilloscope. System B: XRD-31 and 1/2-inch air heliax (30 ns) into a TSN-660; C: XRD-31 and 1/2-inch air heliax (90 ns) into a direct-access Tektronics 7912, D: XRD-31 and 1/2-inch air heliax (90 ns) into an amplified Tektronics 7912.

6. Theoretical fits to x-ray filter transmission data using the FEAF VAX computer processing routine. Data are from the Ionac facility at the LLNL X-ray Calibration and Standards Laboratory.

7. Typical XRD quantum efficiencies measured at the LLNL X-ray Calibration and Standards Laboratory. The smooth curves are normalized values of $E\mu(E)$, where E is the x-ray energy and $\mu(E)$ is the photo-ionization cross section, from Henke, et al.[10]

8. X-ray reflectivity measurements of two grazing incidence, carbon mirrors used for our boron-filtered channels. Data for all our mirrors were obtained by Koppel and Isaacson at the LLNL Ionac.[5] Theoretical values calculated using the REFLECT2 code have been scaled by 0.86 to obtain the best fit.

9. Beryllium x-ray mirror reflectivity values measured at the Ionac fit using REFLECT2 assuming a composition of beryllium and beryllium oxide.

10. Ionac x-ray reflectivity data for a carbon mirror at 2.4^{0} fit with calculated values scaled by 0.82. This mirror is used for one of the vanadium L-edge (0.52 keV) filtered channels.

11. Absolute energy response of a typical carbon K-edge channel obtained using a set of calibrated parylene-N filters, an aluminum XRD and the fit to the Be mirror reflectivity data shown in Fig. 9.

12. Absolute response of a vanadium channel obtained using calibrated vanadium filters, an Al XRD, and the carbon mirror data shown in Fig. 10.

13. Absolute response of a ~700 eV channel consisting of two cobalt filters, and an aluminum XRD. Note the high transmission through the parylene pre-filter used in all Novette Dante channels.

14. Calibrated energy sensitivities of Dante-H channels with filter edges below 800 eV.

15. Calibrated energy sensitivities of Dante-H channels with filter edges above 700 eV.

16. Normalized responses of Novette SDSS channels obtained using an array of grazing incidence mirrors, corresponding K-or L-edge filters, and a gold transmission cathode.

17. Energy response comparisons of channels common to the SDSS and Dante spectrometers showing very good agreement in all cases.

18. Experimental conditions for a Novette 1-ns, 0.53-μm irradiation of a gold disk target.

19. A pinhole-imaged SDSS streak record of the gold disk irradiation described in Fig. 18. SDSS, functioning as a 10X microscope, has an edge-on view of the 200 eV x-ray emission from the disk target. Target is irradiated from the right. Spatial and time axes are the horizontal and vertical axes, respectively. Note general direction of blow-off of emission region as time progresses.

20. This is an isodensity plot of the photo-densitometered streak record in Fig. 19. The compressed and parallel isodensity contour lines around ∿ 1000 μm are an instrumental artifact due to the edge location of the streak camera entrance slit.

21. Temporal profile of 200 eV x-ray emission obtained from a lineout of the contour plot at the spatial position, x=560 μm. The amplitude is obtained from film exposure using a calibrated wedge.

22. Temporal profile of 200 eV x-ray emission at 650 μm.

23. Temporal profile of 200 eV x-ray emission at 710 μm.

24. Temporal profile of 200 eV x-ray emission at 780 μm.

25. Temporal profile of 200 eV x-ray emission at 930 μm.

26. Representative normalized oscilloscope pulses for several Dante-A channels showing a gradual decrease in the FWHM of the spatially integrated, disk spectral emission time with increasing x-ray energy. Signals have been aligned at their leading edges. A. Boron (edge energy = 0.19 keV), B. C-H (0.28 keV), C. Vanadium (0.52 keV), D. Iron (0.71 keV), E. Copper (0.93 keV), F. Magnesium (1.30 keV).

27. Dante-A channel energy responses and integrals of normalized response times-final spectrum for all Dante-A channels. The spectral points are plotted at the 50% values of these integral curves.

28. Prompt low energy, x-ray gold disk spectrum unfolded from Novette Dante-A oscilloscope data using the UNSPEC code. The points show the channel-to-channel deviations of the spectrum from the smooth curve that best fits the data.

References

1. For the development of these instruments see, for example, "Diagnostics Technology", in several Laser Program Annual Reports, Lawrence Livermore National Laboratory, Livermore, CA, UCRL-50021, p. 5-1 (1978 through 1981).

2. K. G. Tirsell, "New Filtered-XRD Low Energy X-ray Spectrometer", Lawrence Livermore National Laboratory, UCID-19394, (May 1982).

3. G. L. Stradling, D. T. Attwood, and R. L. Kauffman, "A Soft X-ray Streak Camera", IEEE Journal of Quantum Electronics, QE-19, 604 (1983) and R. L. Kauffman, G. L. Stradling, D. T. Attwood, and H. Medecki, "Quantitative Intensity Measurements Using a Soft X-Ray Streak Camera", IEEE Journal of Quantum Electronics, QE-19, 616, (April 1983).

4. N. M. Ceglio, M Roth, A. M. Hawryluk, "A Streaked, X-ray Transmission Grating Spectrometer", in Proceedings of Low Energy X-ray Diagnostics-1981, Monterey, D. T. Attwood and B. L. Henke, Eds., p. 290, (AIP, New York, 1981).

5. K. G. Tirsell, D. G. Nilson, J. M. Auerbach, T. G. Woehrle, R. M. Penparaze (LLNL), and L. N. Koppel, C. E. Isaacson (Aracor Co.), "Absolute Calibration of Filtered X-Ray Diode Systems With Grazing Incidence Mirror Cutoffs", Lawrence Livermore National Laboratory, UCRL-89501, to be published.

6. J. M. Auerbach with the aid of B. J. De Martini and R. W. Carey, LLNL, has developed VAX computer routines to process our calibration data. Also see K. G. Tirsell and J. M. Auerbach, "X-ray Filter-Transmission Data Processing", Laser Program Annual Report, UCRL-50021-82, p. 5-3, to be published.

7. Instead of Formvar, we now use parylene-N for the Dante carbon K-edge filter and carbon for the SDSS carbon K-edge filter. We continue to calibrate and use Formvar foils made at LLNL for proportional counter windows.

8. K. G. Tirsell, "Absolute Photoelectric X-Ray Diode Sensitivity", Laser Program Annual Report, UCRL-50021-81, p. 5-8 (1981). For a good review of LLNL x-ray calibration methods see J. L. Gaines, "Low Energy X-Ray Calibration Sources at the Lawrence Livermore National Laboratory" in Proceedings of Low Energy X-ray Diagnostics-1981, Momterey, D. T. Attwood and B. L. Henke, Eds., p. 246. (AIP, New York, 1981).

9. J. L. Gaines, "A Generator for Producing Monoenergetic, High Intensity, Soft X-Rays", Nuclear Instruments and Methods 102, 7 (1972).

10. B. L. Henke, P. Lee, T. J. Tanaka, R. L. Shimabukuro and B. K. Fujikawa, "Low Energy X-Ray Interaction Coefficients: Photoionization, Scattering and Reflection," Atomic Data and Nuclear Data Tables 27, No. 1, (1982).

11. B. L. Henke, J. P. Knauer and K. Premaratne, "The Characterization of X-Ray Photocathodes in the 0.1-10 keV Photon Energy Region", J. of Appl. Phys. 52, 1509 (1981).

12. H. F. Finn, "REFLECT1 and REFLECT2", unpublished LLNL memo CPG-77-125, (Nov. 15, 1977).

13. A. Toor, LLNL, private communication (1983).

14. H. F. Finn, "UNSPEC Reference Manual Version 10/29/82", unpublished LLNL Report, UCID-19616, (December 1, 1982).

15. P. H. Y. Lee and K. G. Tirsell, "X-ray Conversion Efficiency", in Laser Program Annual Report, Vol. 2, LLNL, Livermore, CA, UCRL-50021-80, p. 7-10 (1980).

Fig 1

Novette target chamber

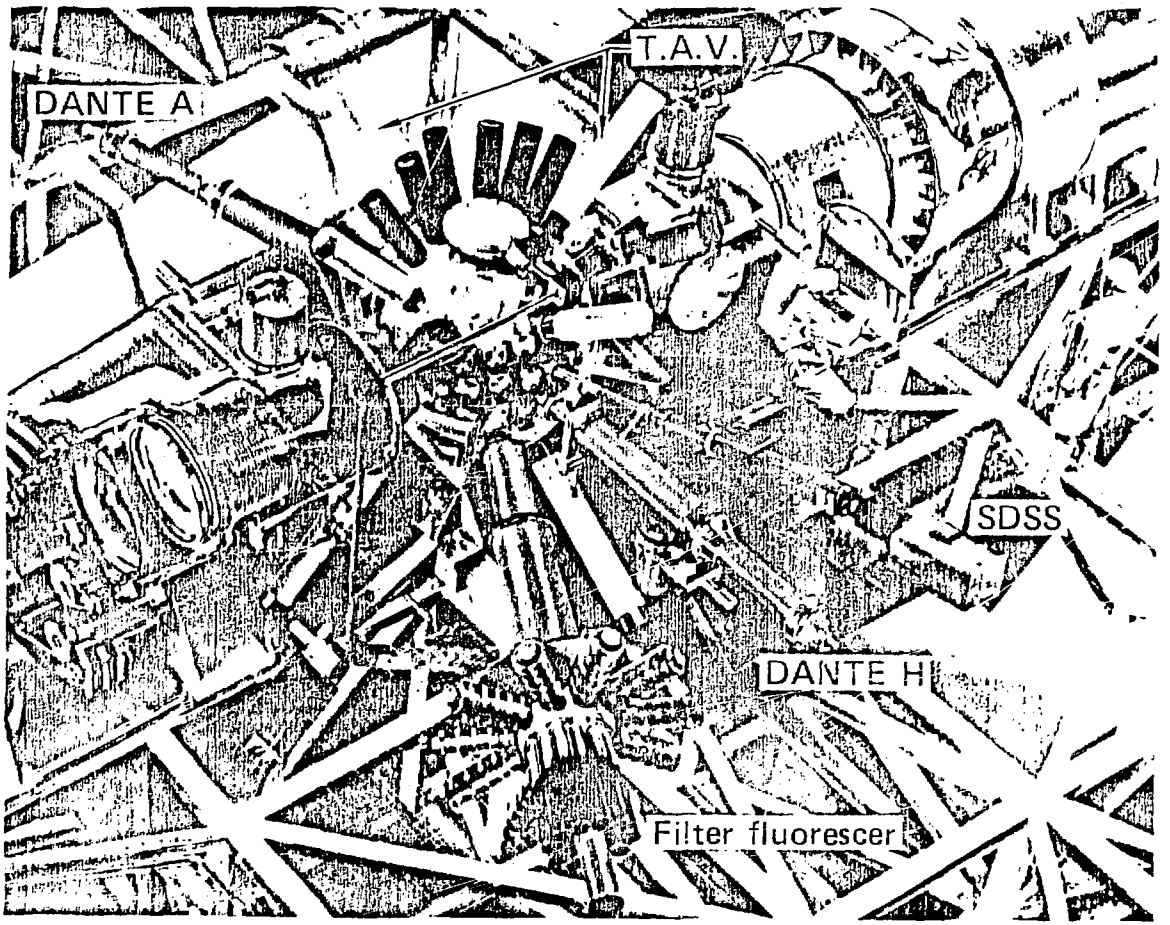

02 32-0582-1908A

Fig 2

Ten-channel Novette filtered x-ray diode system

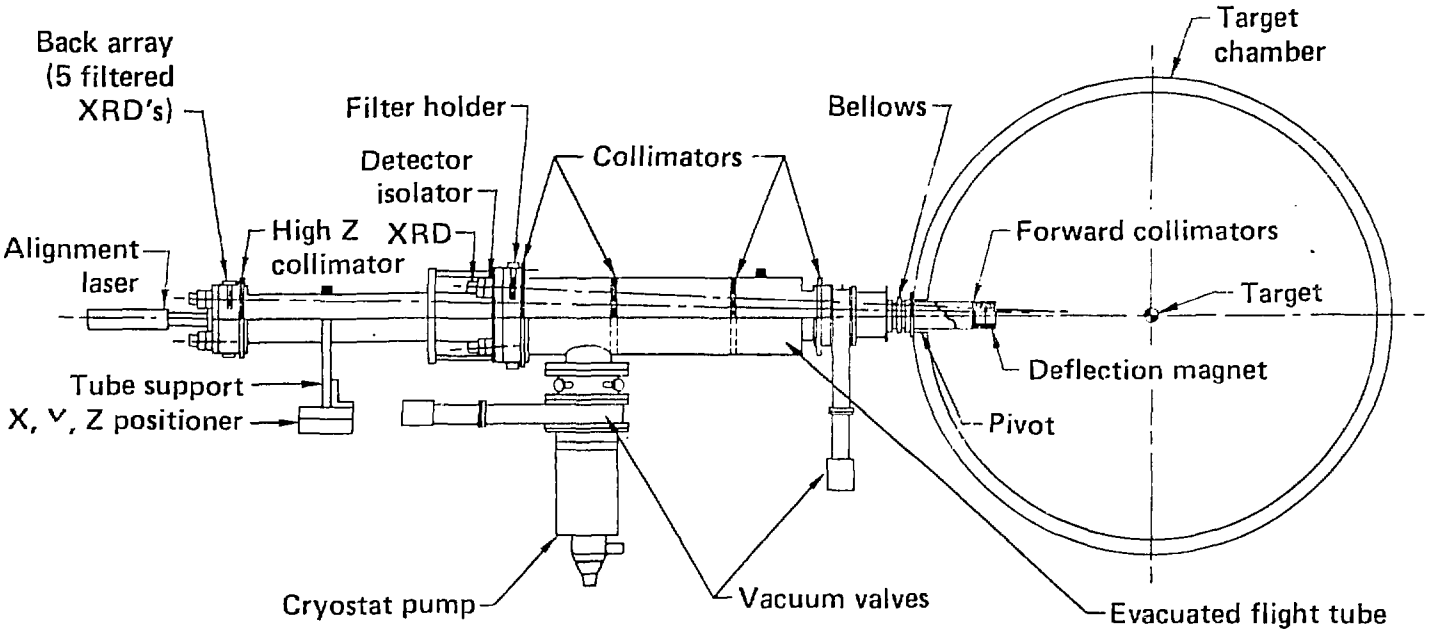

Fig 3

Typical mirror "Dante" channel

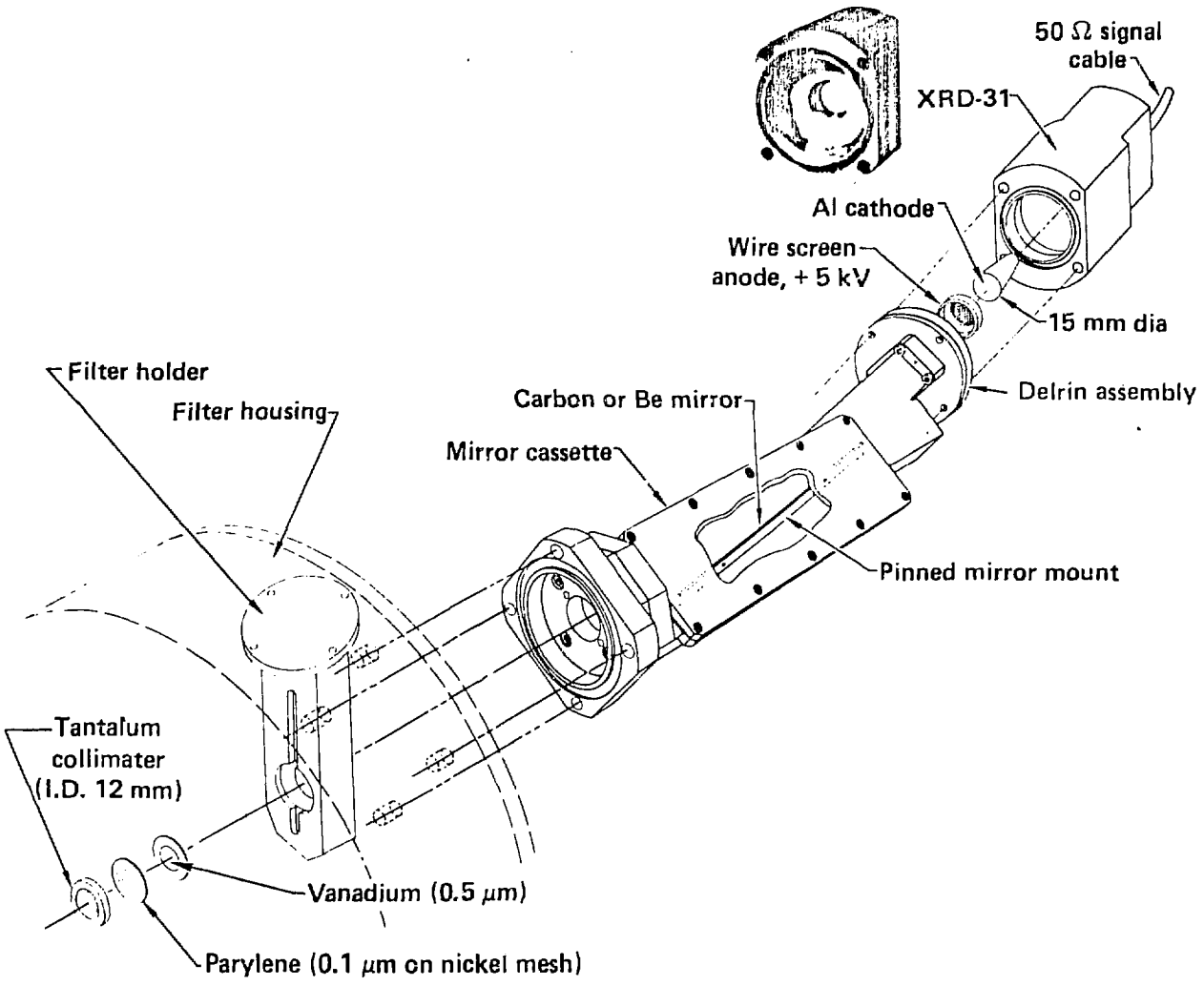

Fig 4

Multi-channel reflector-filter soft x-ray streak camera

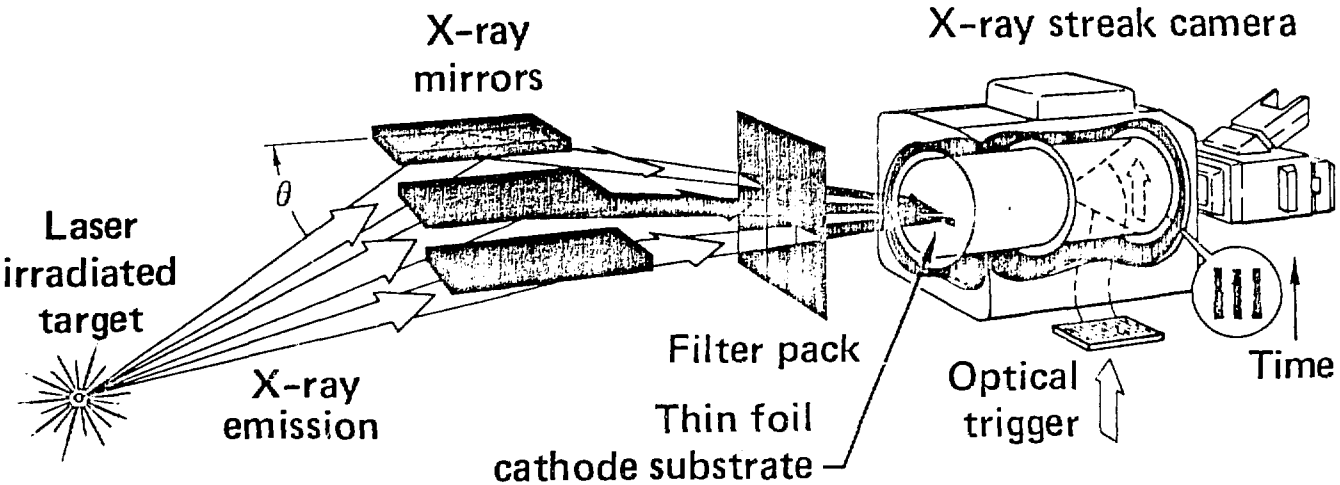

40-01-1278-4604A

System impulse time responses including XRD, cable and oscilloscope

	System		FWHM	Rise time (10-90)%	Fall time (90-10)%
	Detector	Scope	ps	ps	ps
	50 ps	TSN-660	< 120	< 100	< 120
	XRD-31	TSN-660	135	110	–
·—	XRD-31	DA-7912	335	305	430
– –	XRD-31	Amp-7912	730	585	505

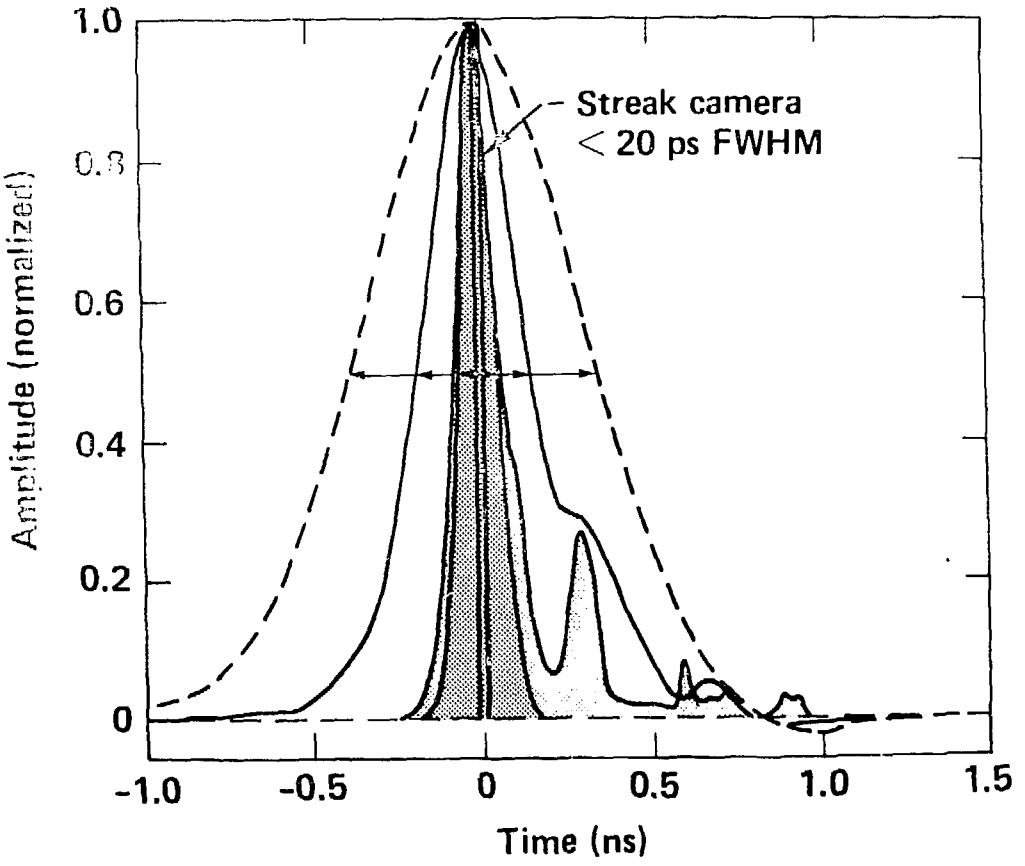

Fig 6

Typical filter transmission calibrations

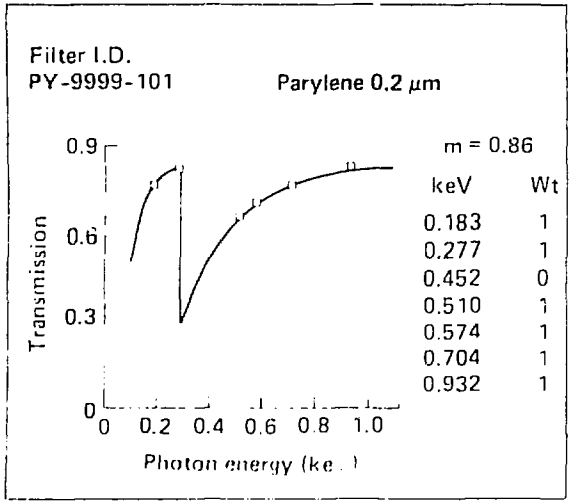

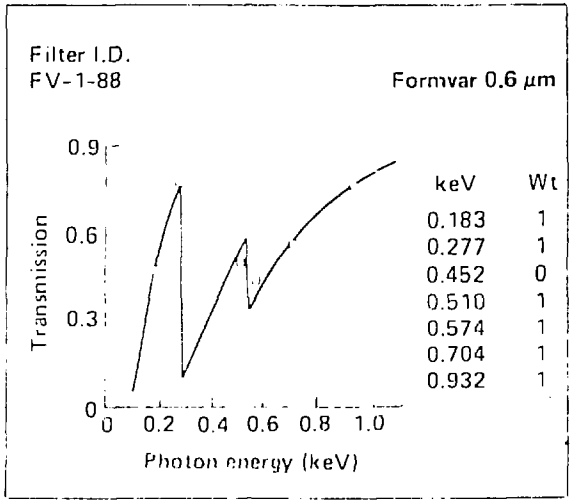

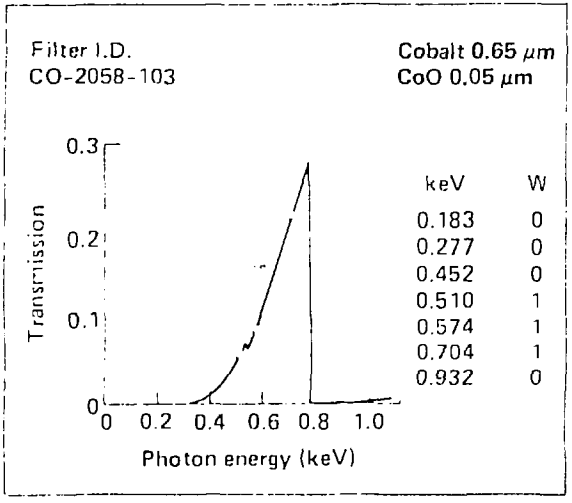

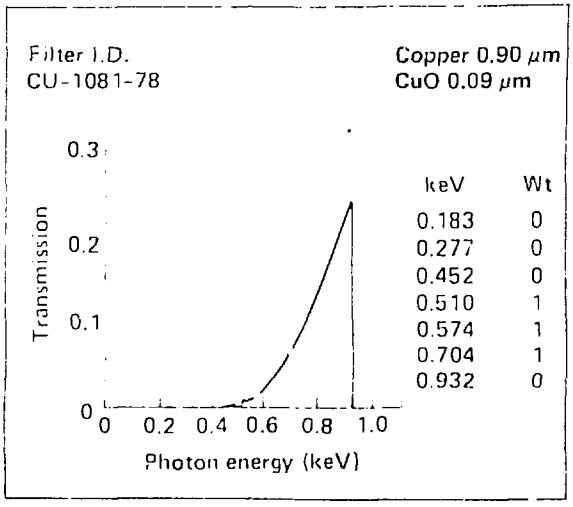

20-01-0883-3321

Calibrated XRD quantum efficiencies vs Eμ (E) model

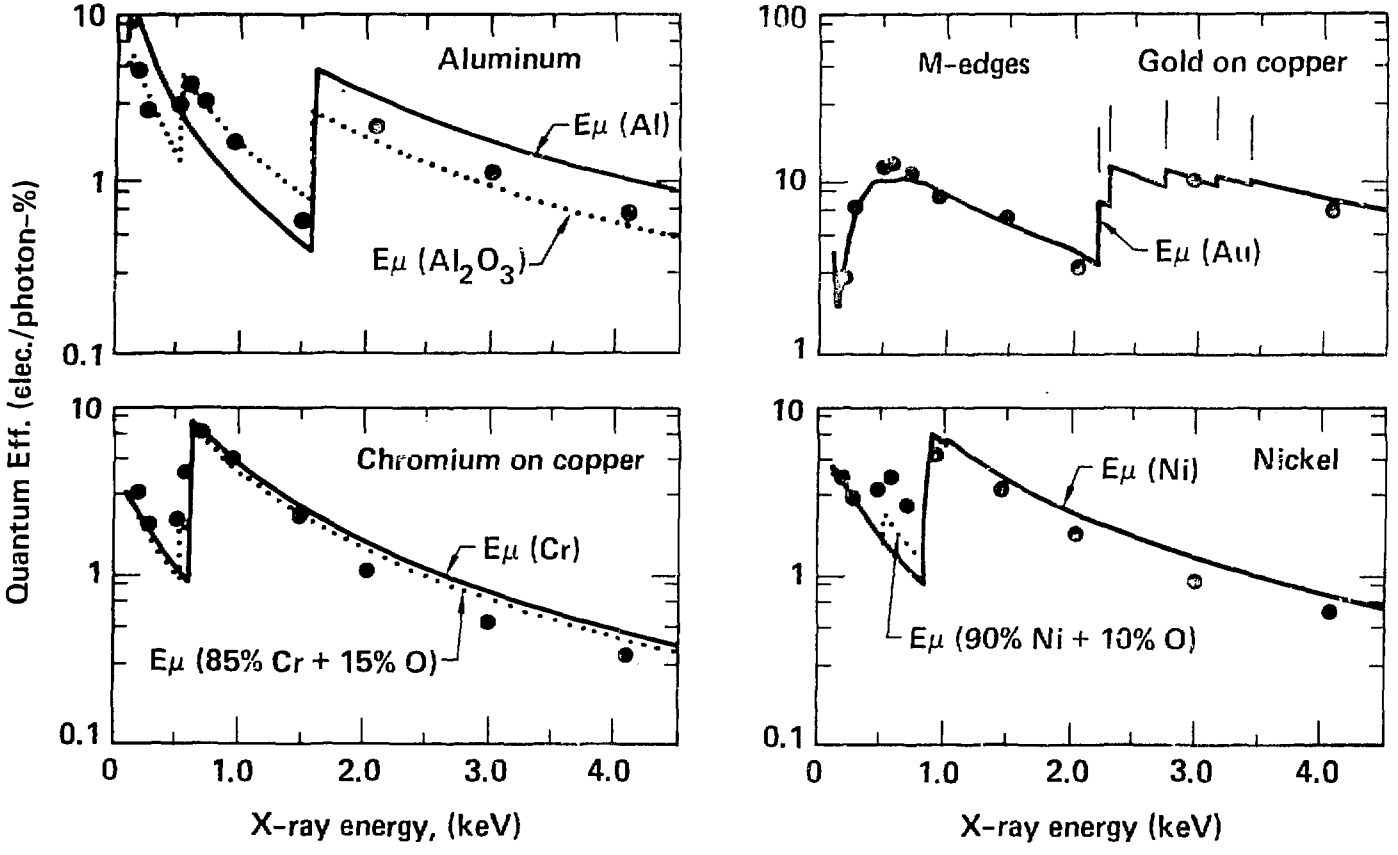

Fig 8

X-ray mirror reflectivity calibrations
5 degree carbon mirrors for boron channels

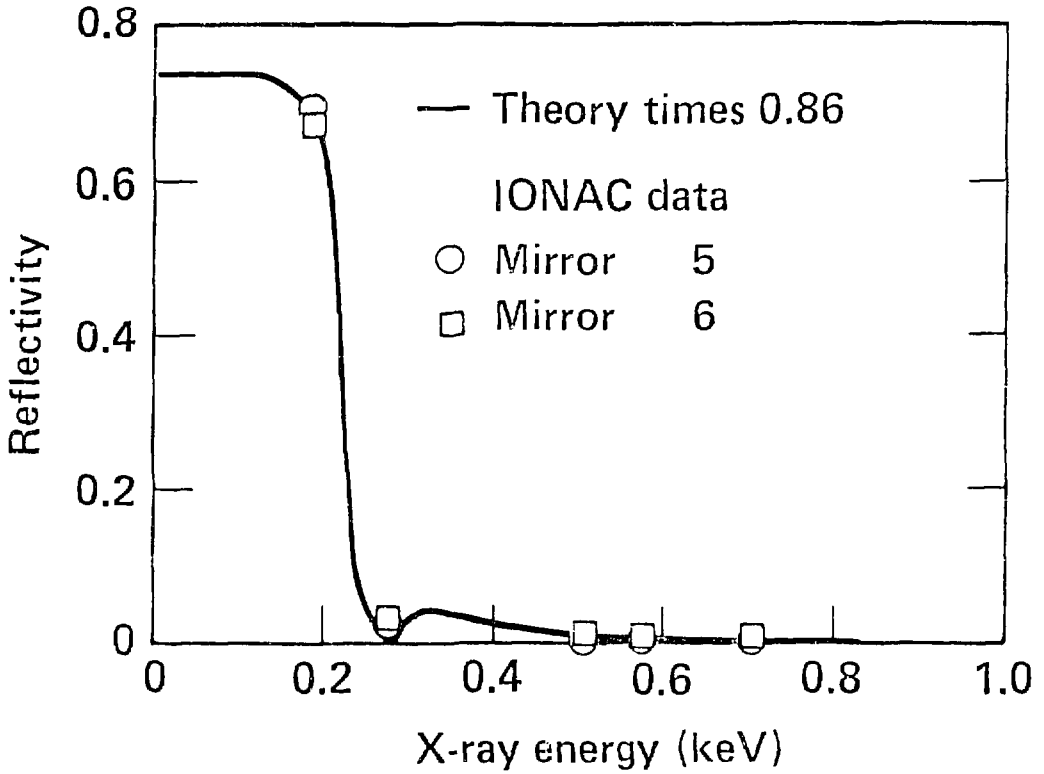

20-50-0883-3327

Fig 9

X-ray mirror reflectivity calibrations
3.4 degree beryllium mirrors for parylene channels

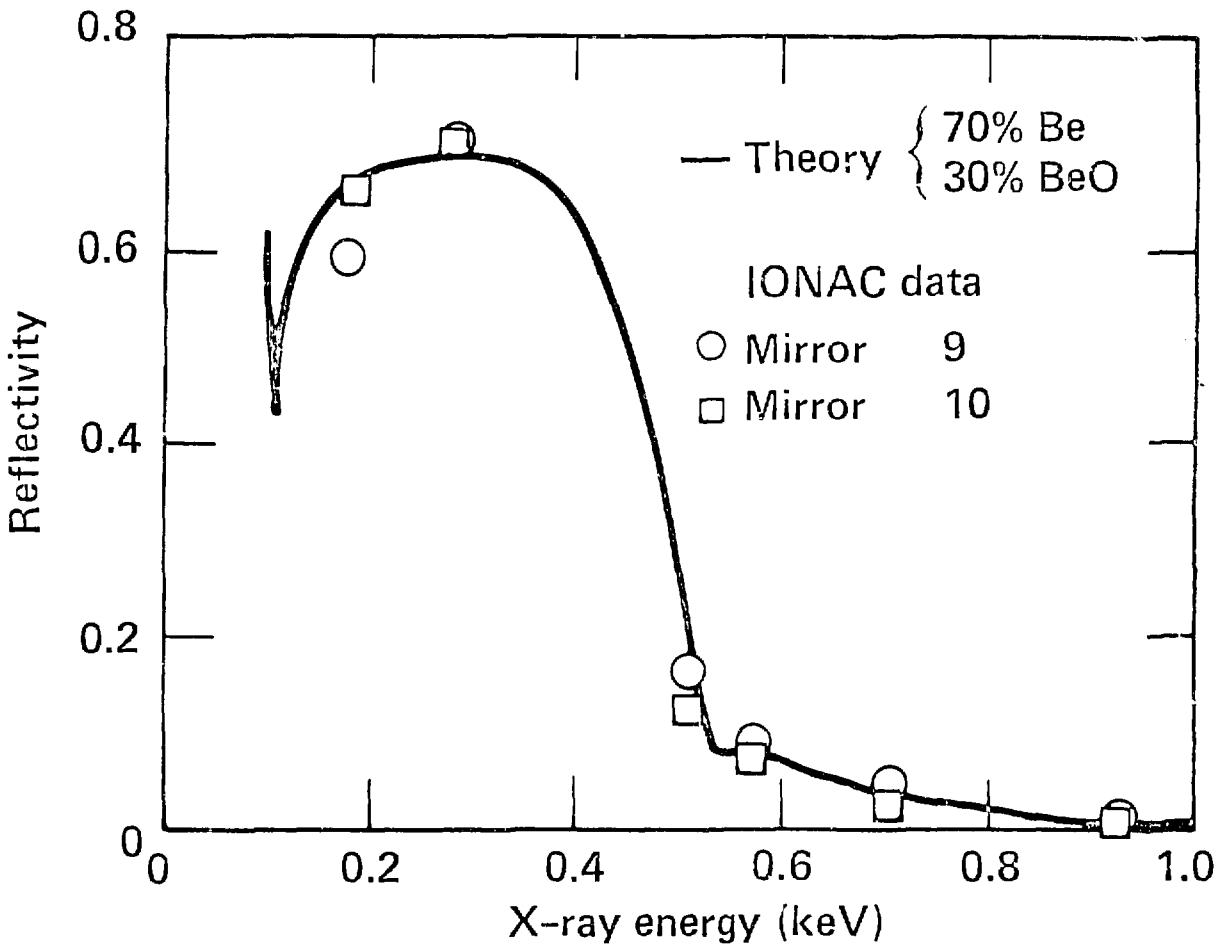

20-50-0883-3325

Fig 10

X-ray mirror reflectivity calibration
2.4 degree carbon for vanadium channels

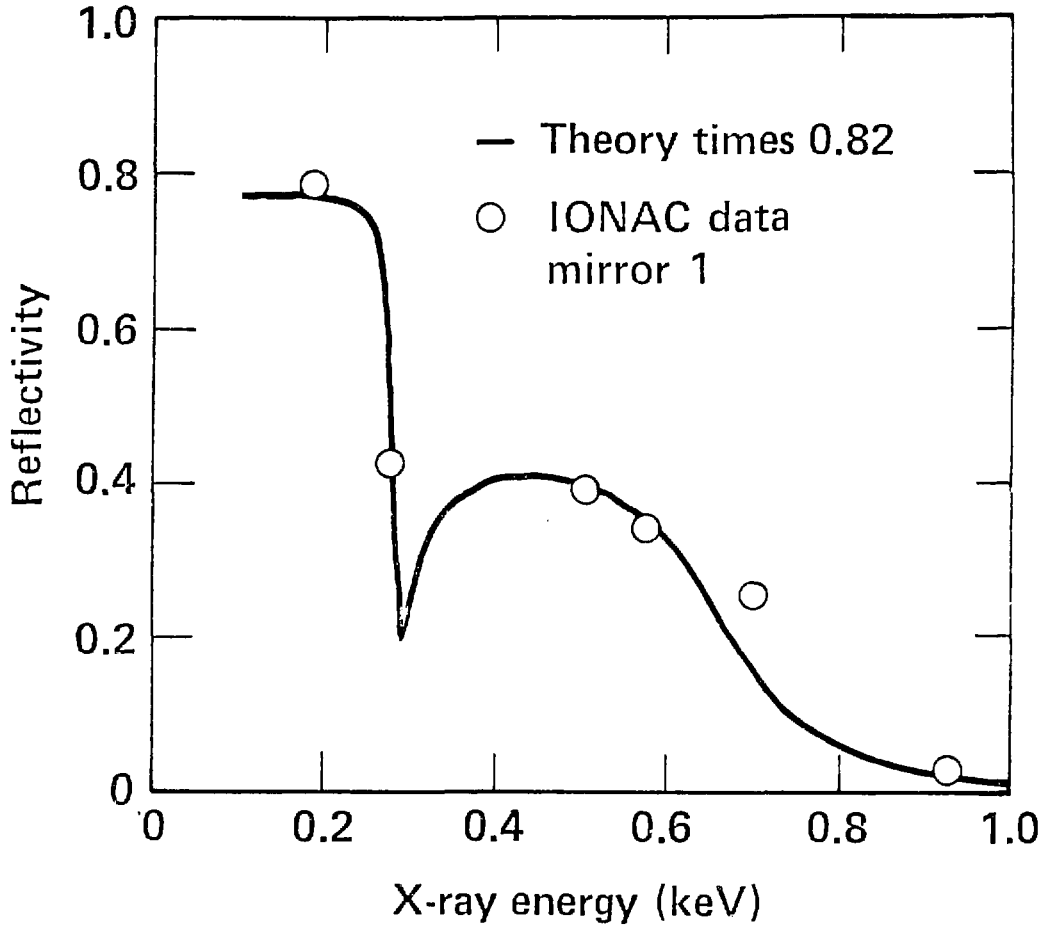

20-50-0883-3326

Dante x-ray channel response
Novette parylene-filtered channel

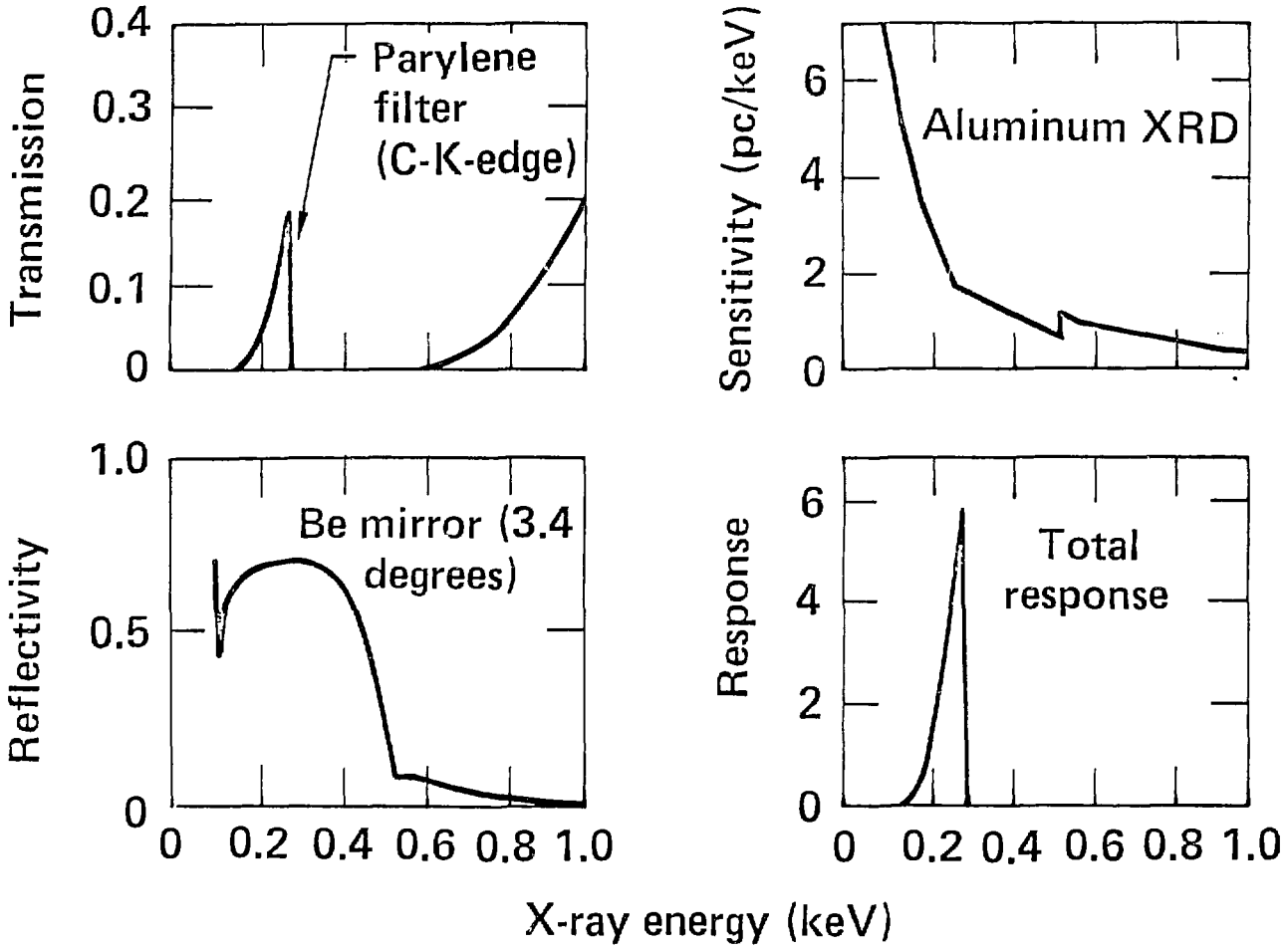

Fig 12

Dante x-ray channel response
Novette vanadium-filtered channel

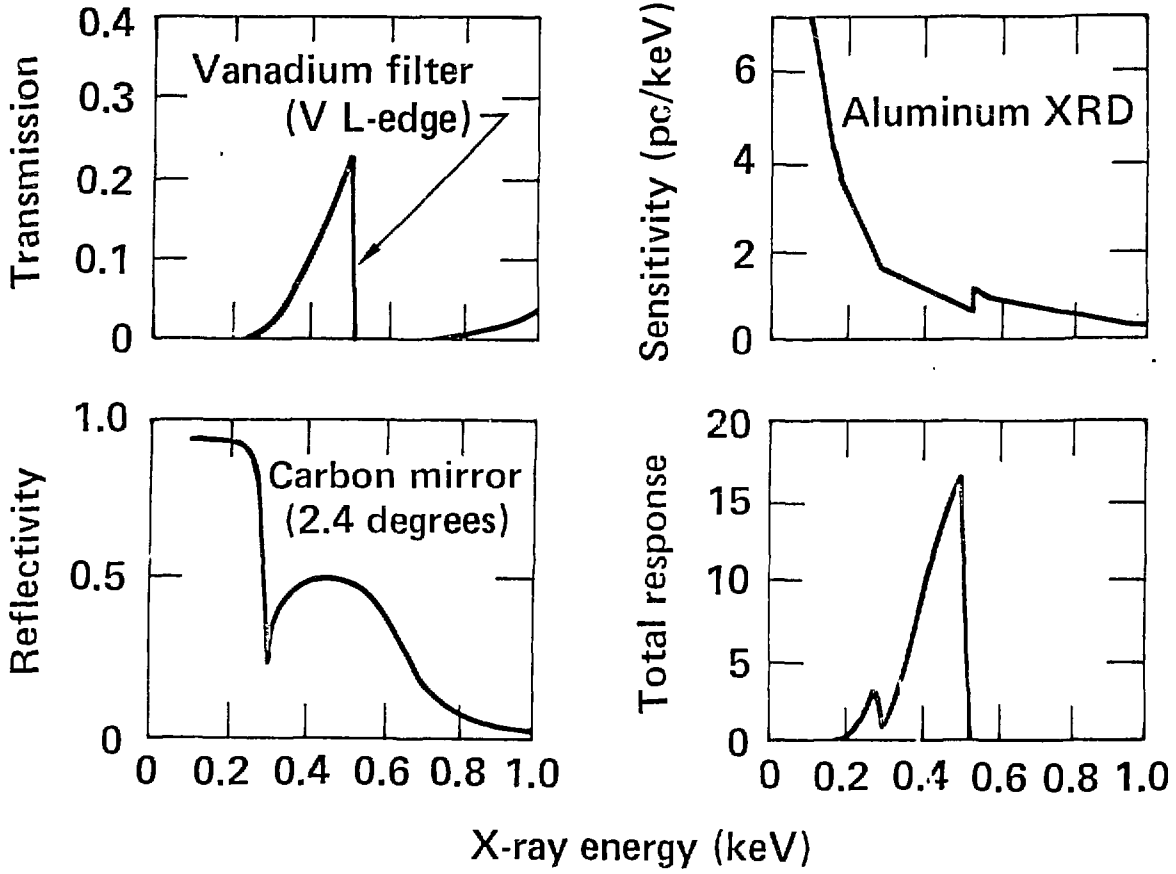

20-50-0883-3322

Dante x-ray channel response
Novette cobalt-filtered channel

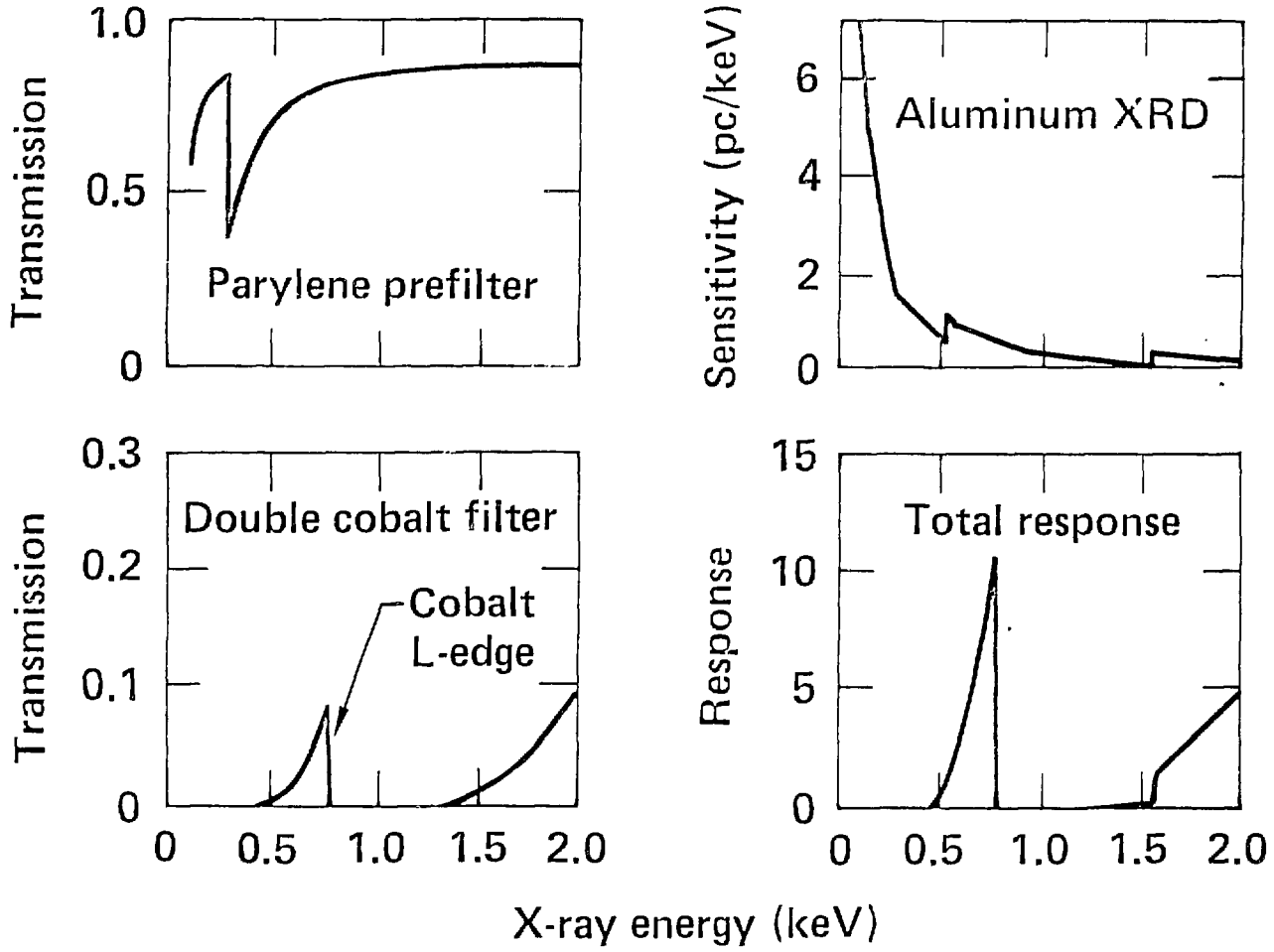

20-50-0883-3324

Not correct

Fig 4

Filtered XRD Channel Sensitivity — Filter edges below 700 eV

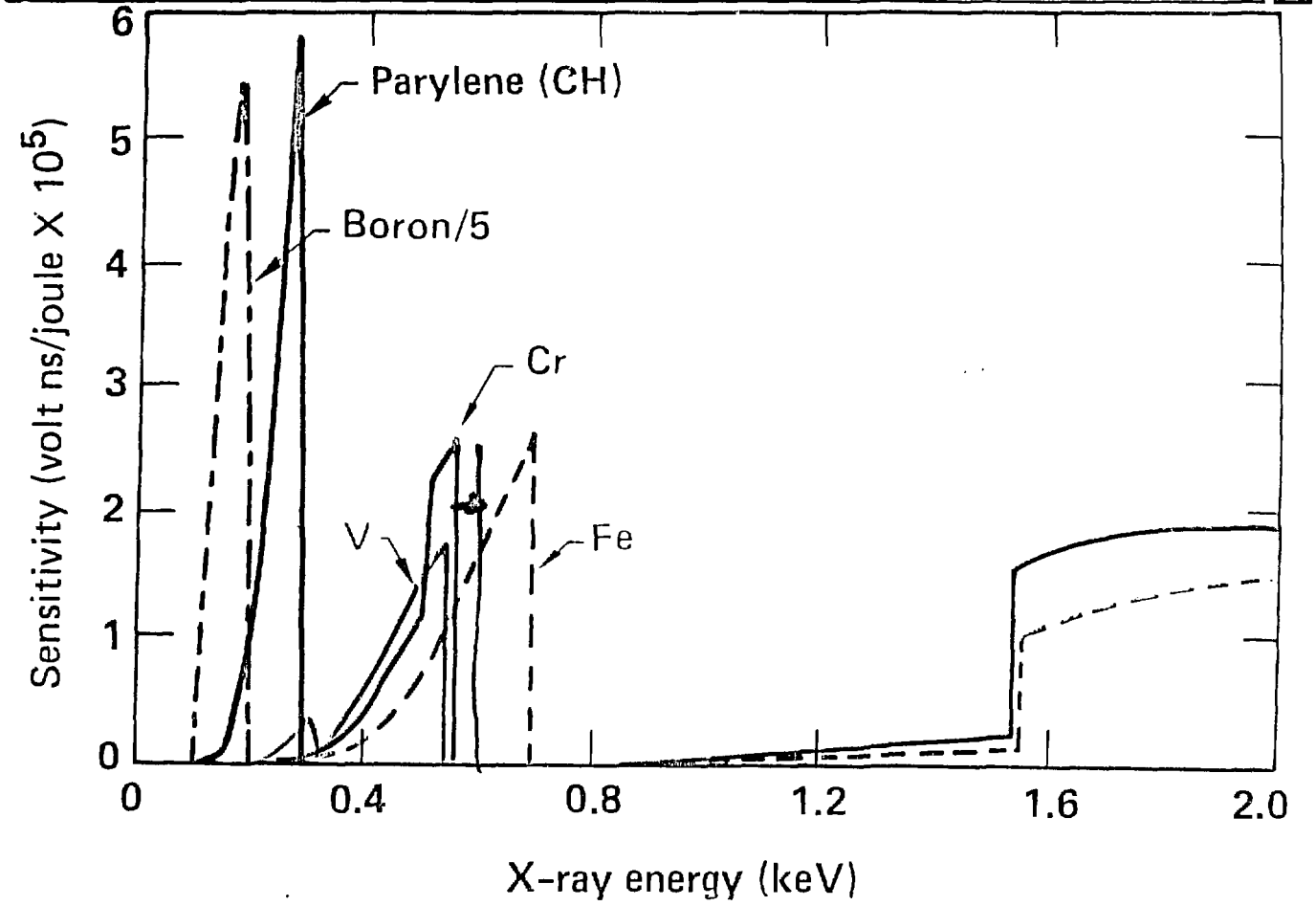

20-01-0883-3309

Fig 15

Filtered XRD Channel Sensitivity — Filter edges above 700 eV

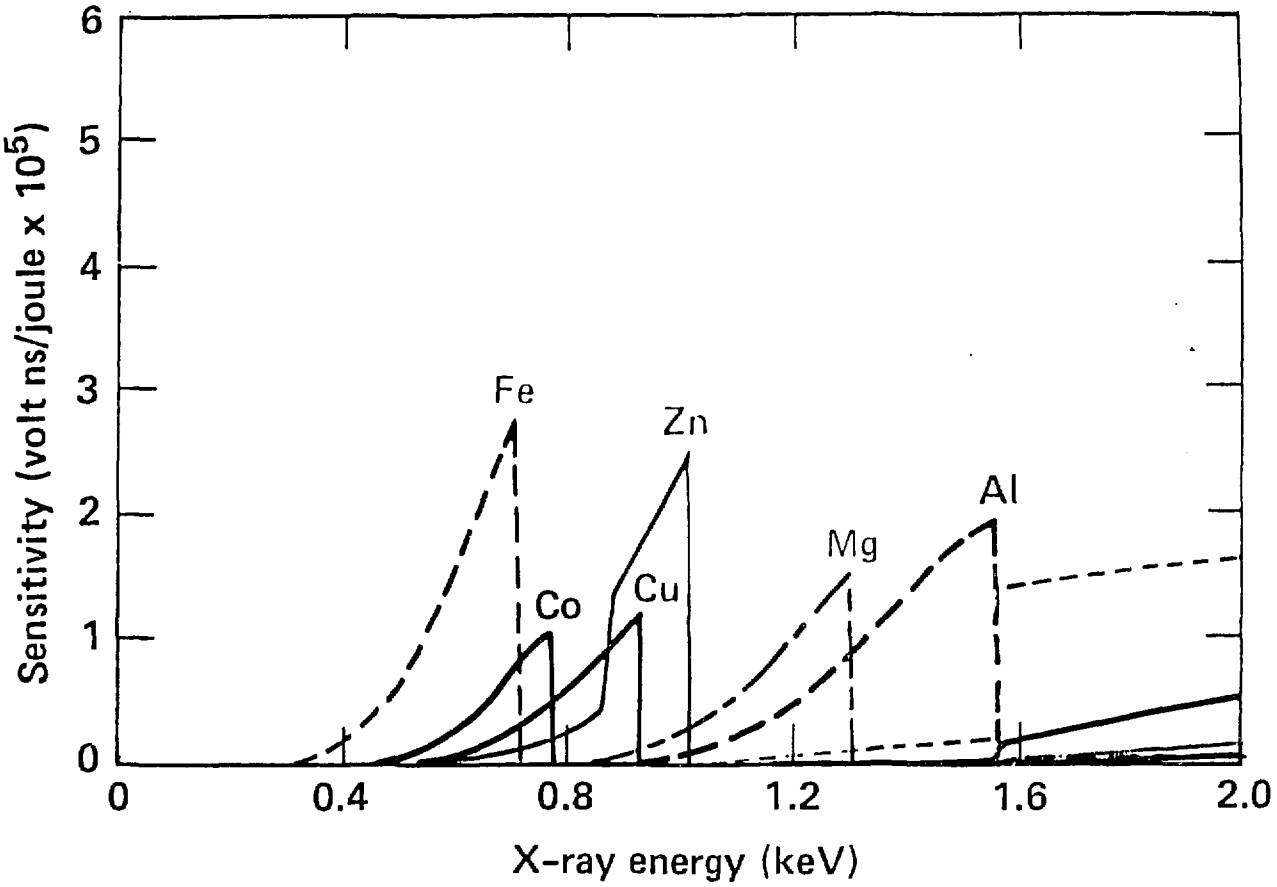

20-01-0883-3308

Fig. 16

Novette SDSS channel responses

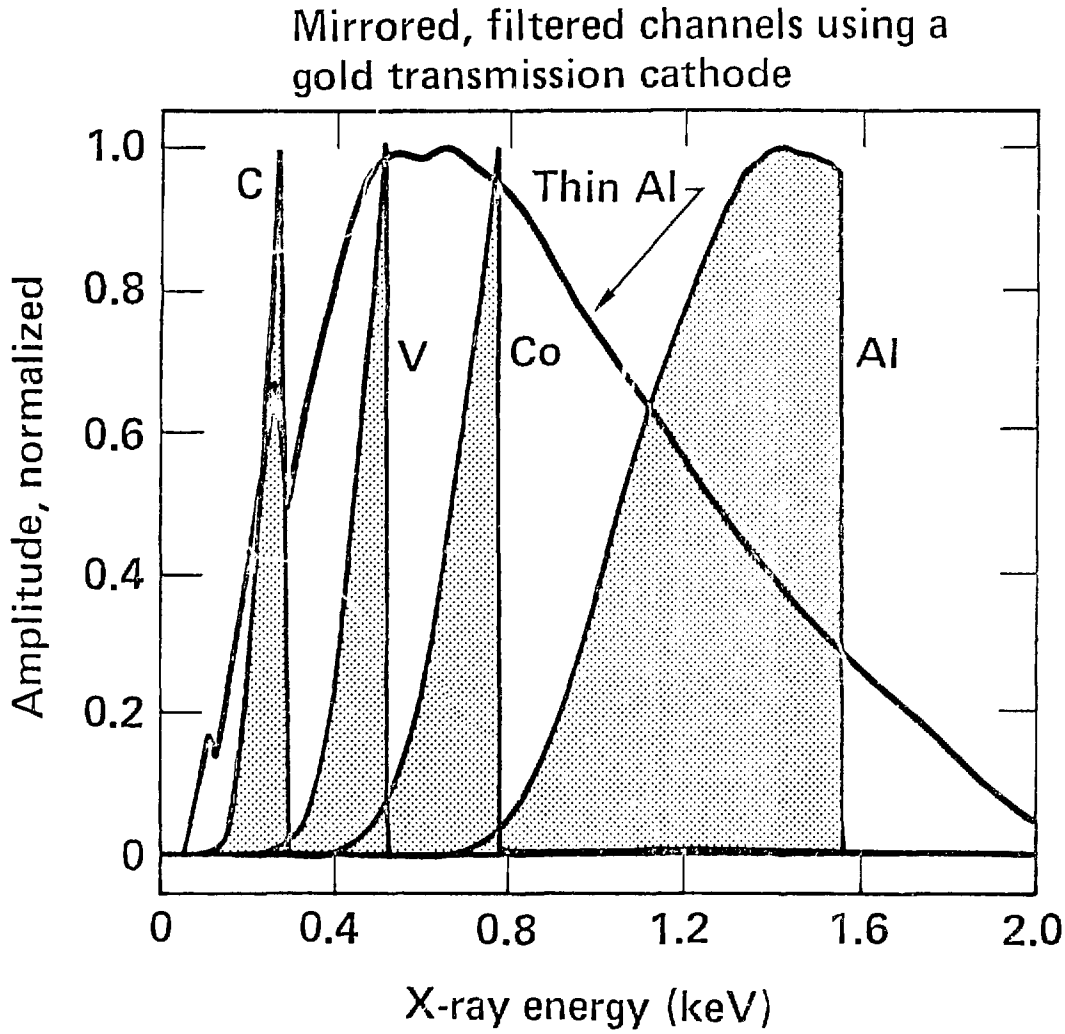

02-32-0883-3328

Fig 1

Matched responses of the two instruments

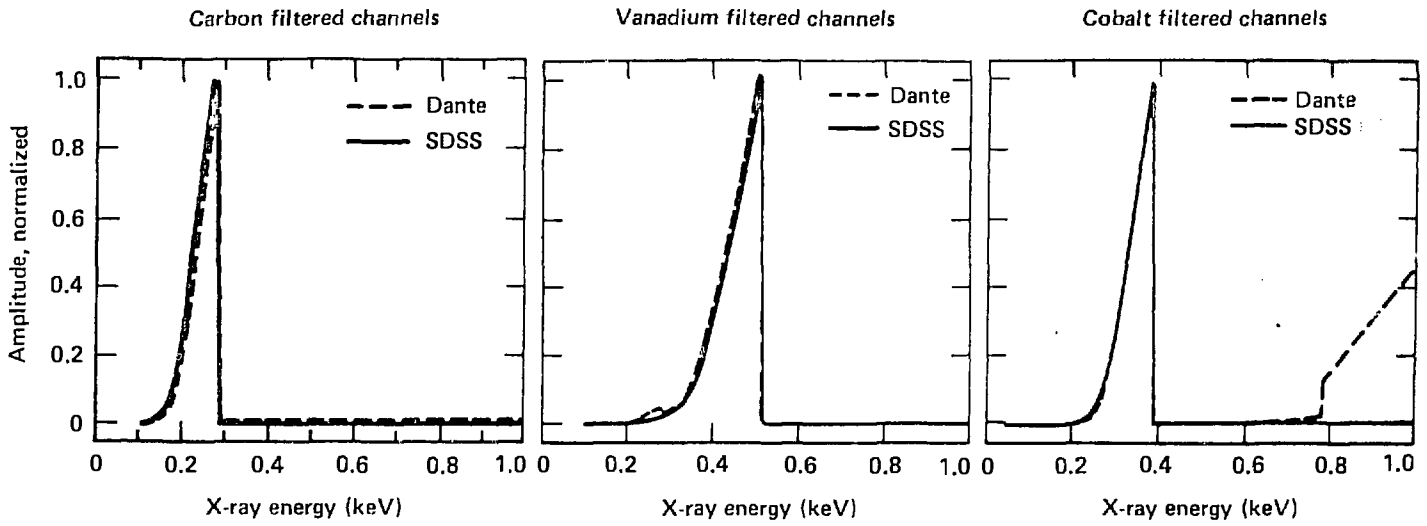

Fig 18

Novette gold disk irradiation experimental conditions

Shot: 93060711
Laser: North Beam
0.53 μm
0.64 kJ, 1 ns FWHM, 3.8E14 W/cm^2
Target: Gold Disk, 1.2 mm diam, 5 μm thick
normal incidence

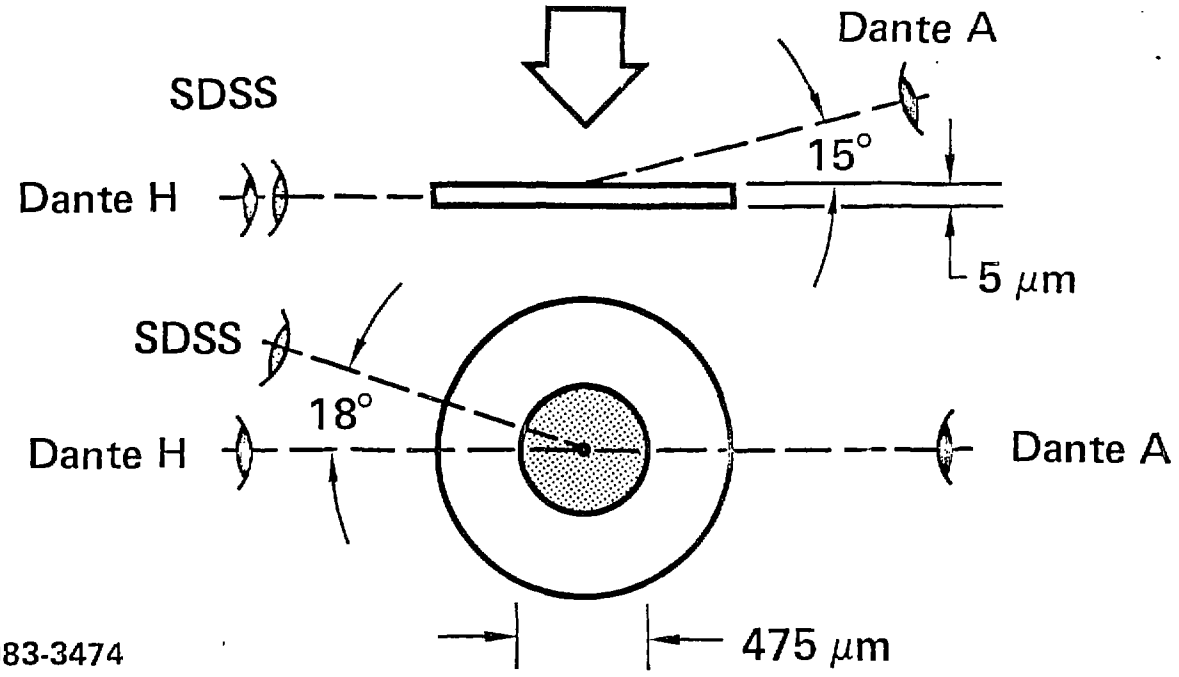

20-01-0983-3474

Fig 1.9

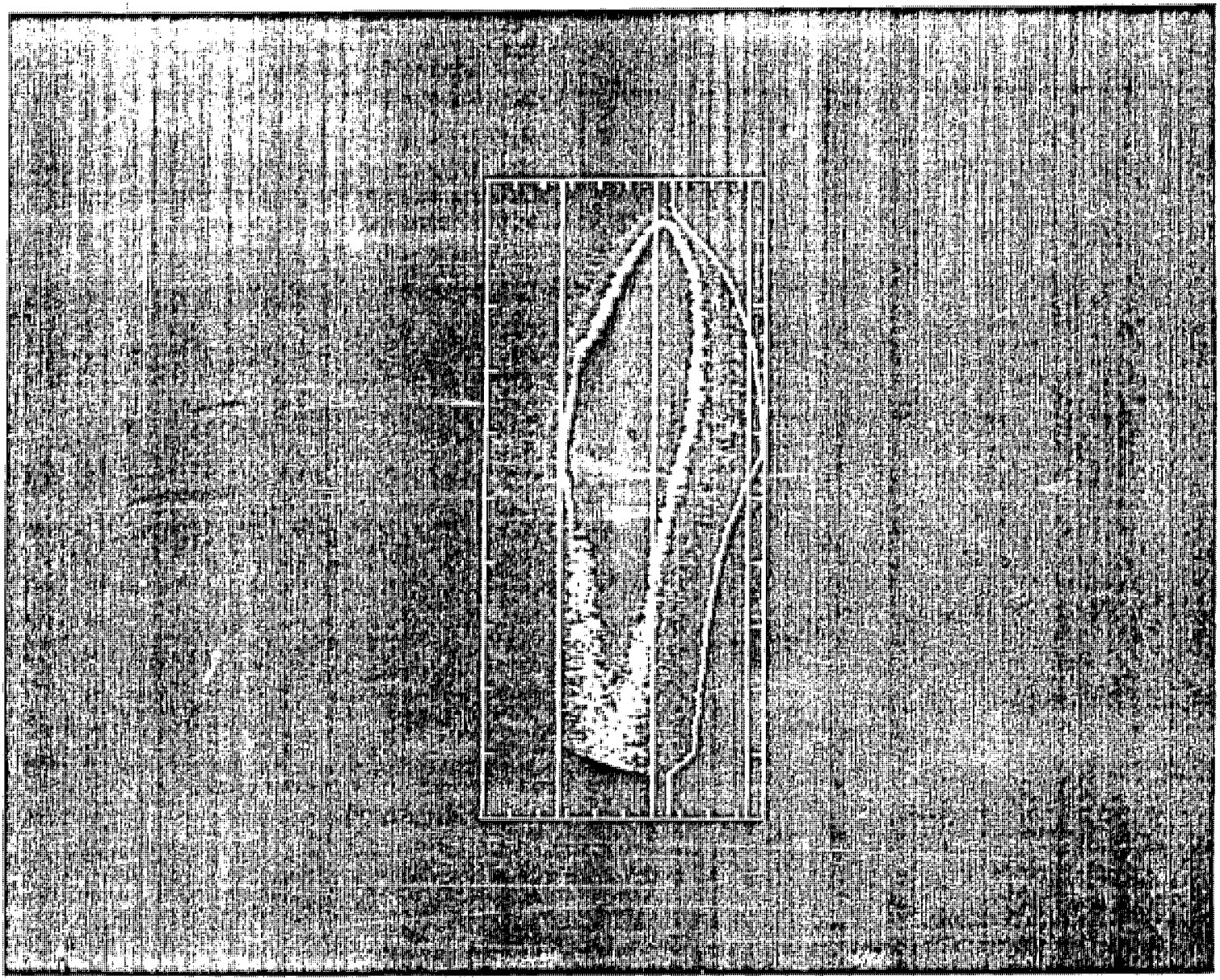

Fig 20

PDS# 93060711SDSS

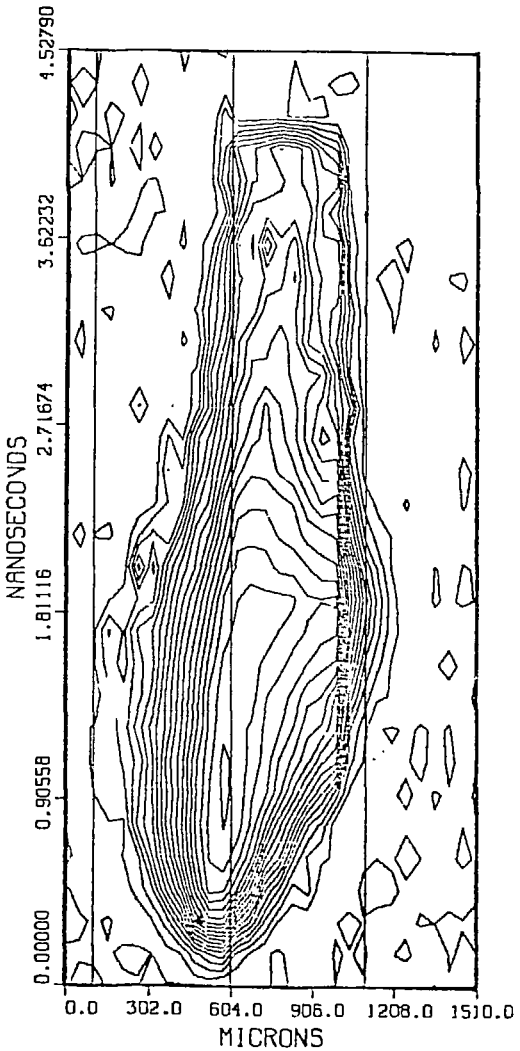

Fig 21

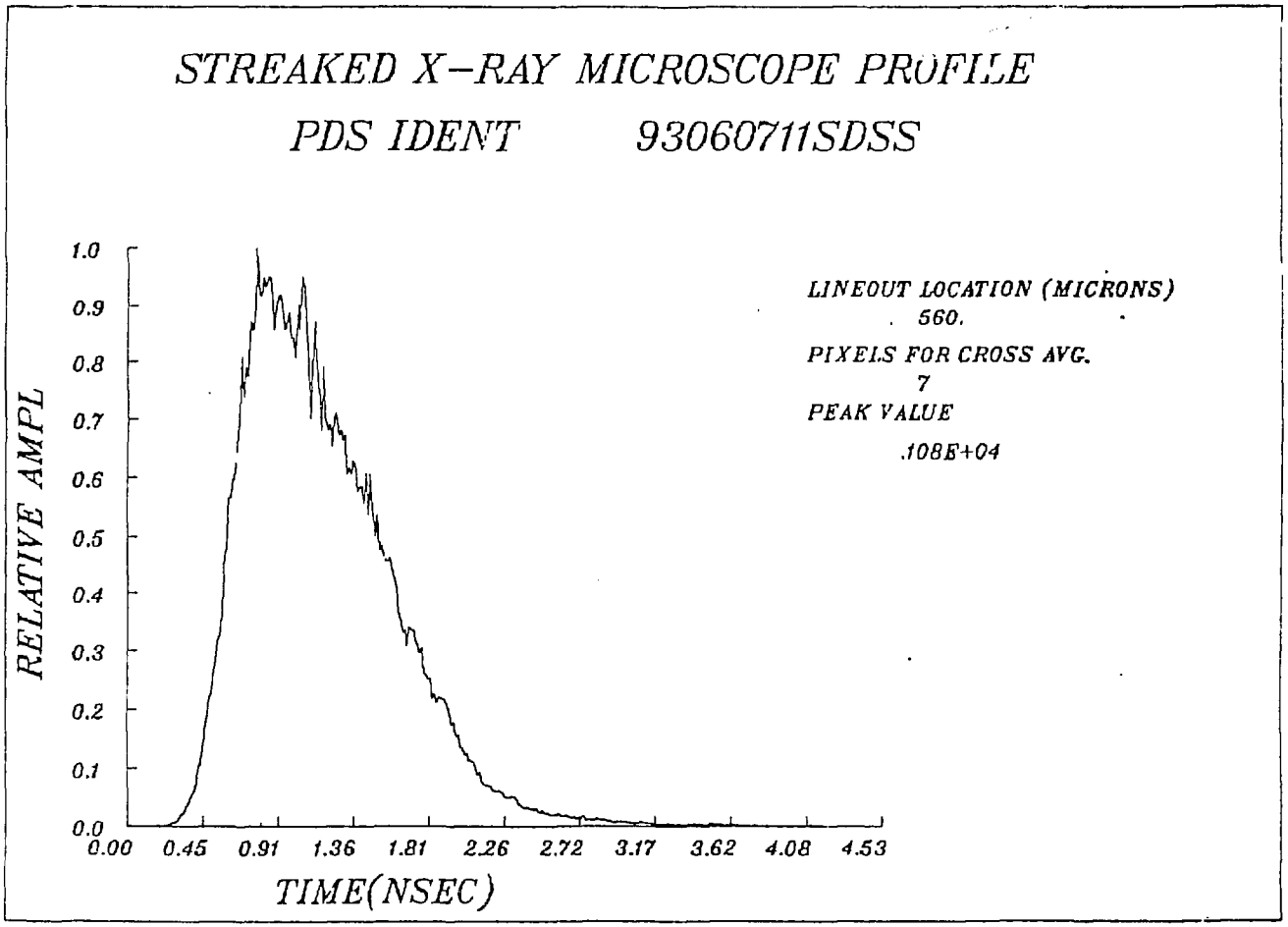
STREAKED X-RAY MICROSCOPE PROFILE
PDS IDENT 93060711SDSS
RELATIVE AMPL
1.0
0.9
0.8
0.7
0.6
0.5
0.4
0.3
0.2
0.1
0.0
0.00 0.45 0.91 1.36 1.81 2.26 2.72 3.17 3.62 4.08 4.53
TIME(NSEC)
LINEOUT LOCATION (MICRONS)
560.
PIXELS FOR CROSS AVG.
7
PEAK VALUE
.108E+04

Fig 22

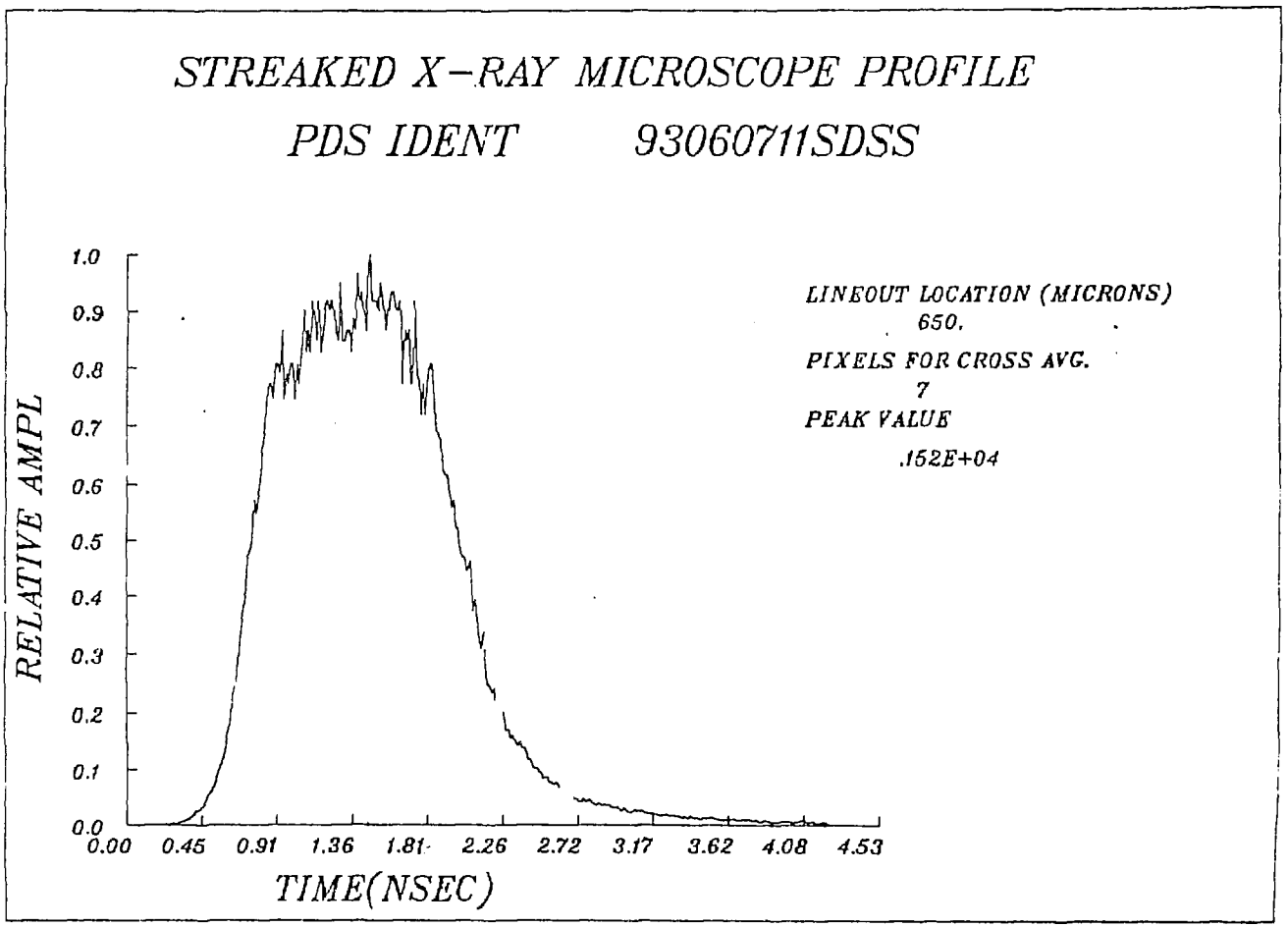
STREAKED X-RAY MICROSCOPE PROFILE
PDS IDENT 93060711SDSS
RELATIVE AMPL
1.0
0.9
0.8
0.7
0.6
0.5
0.4
0.3
0.2
0.1
0.0
0.00 0.45 0.91 1.36 1.81 2.26 2.72 3.17 3.62 4.08 4.53
TIME(NSEC)
LINEOUT LOCATION (MICRONS)
650.
PIXELS FOR CROSS AVG.
7
PEAK VALUE
.152E+04

Fig 23

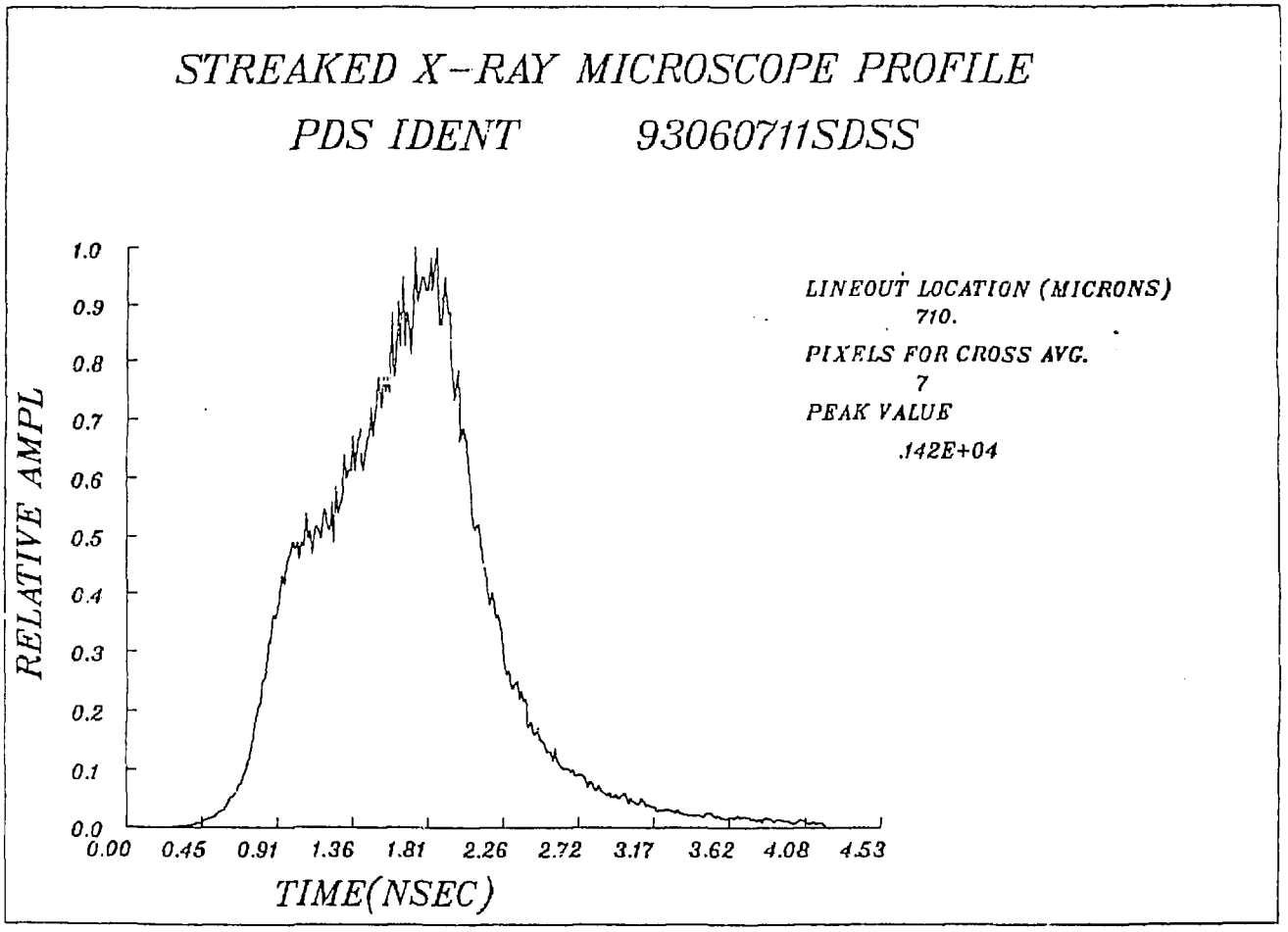
STREAKED X-RAY MICROSCOPE PROFILE
PDS IDENT 93060711SDSS
RELATIVE AMPL
1.0
0.9
0.8
0.7
0.6
0.5
0.4
0.3
0.2
0.1
0.0
0.00 0.45 0.91 1.36 1.81 2.26 2.72 3.17 3.62 4.08 4.53
TIME(NSEC)
LINEOUT LOCATION (MICRONS)
710.
PIXELS FOR CROSS AVG.
7
PEAK VALUE
.142E+04

Fig 24

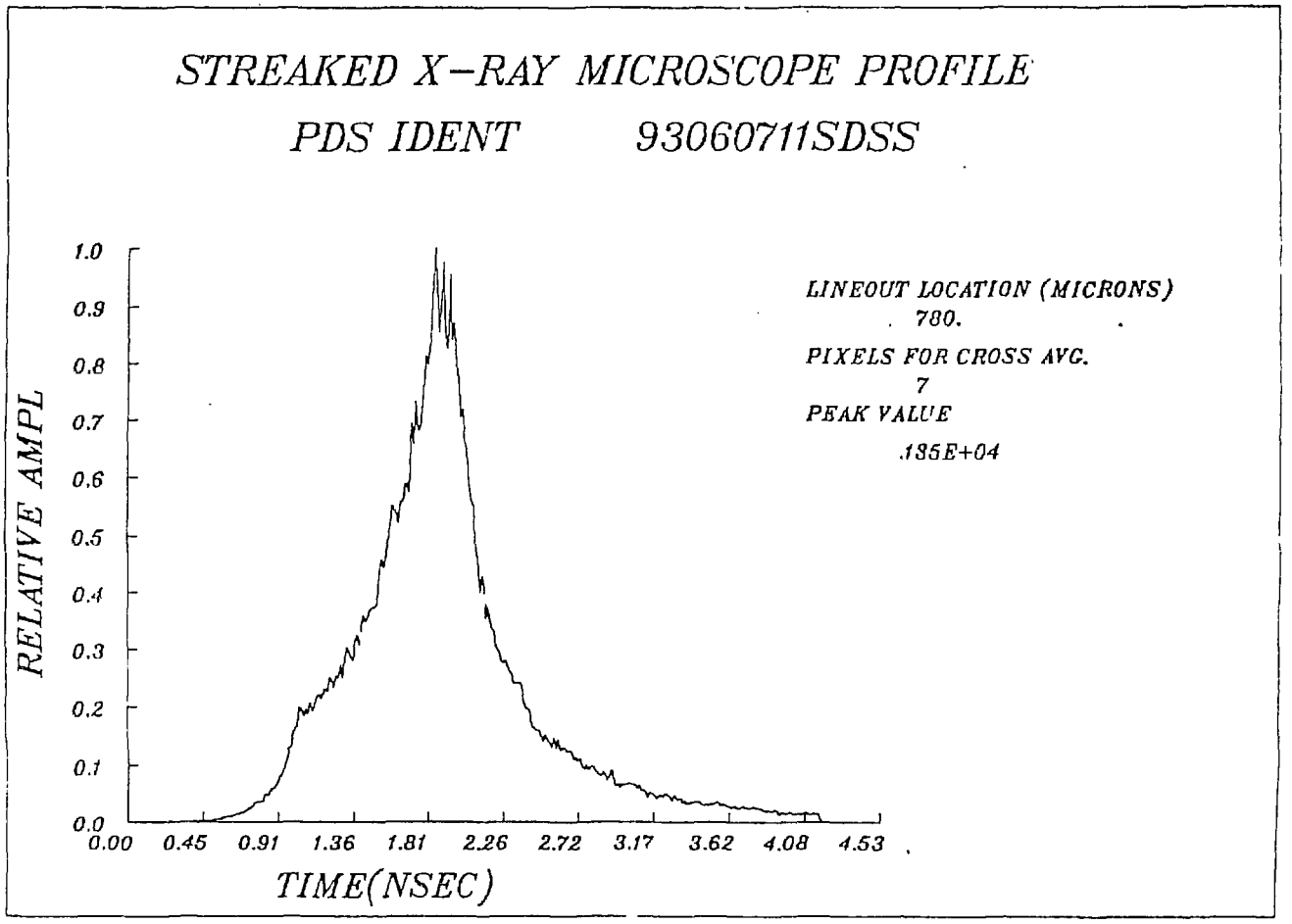
STREAKED X-RAY MICROSCOPE PROFILE
PDS IDENT 93060711SDSS
RELATIVE AMPL
1.0
0.9
0.8
0.7
0.6
0.5
0.4
0.3
0.2
0.1
0.0
0.00 0.45 0.91 1.36 1.81 2.26 2.72 3.17 3.62 4.08 4.53
TIME(NSEC)
LINEOUT LOCATION (MICRONS)
780.
PIXELS FOR CROSS AVG.
7
PEAK VALUE
.185E+04

Fig 25

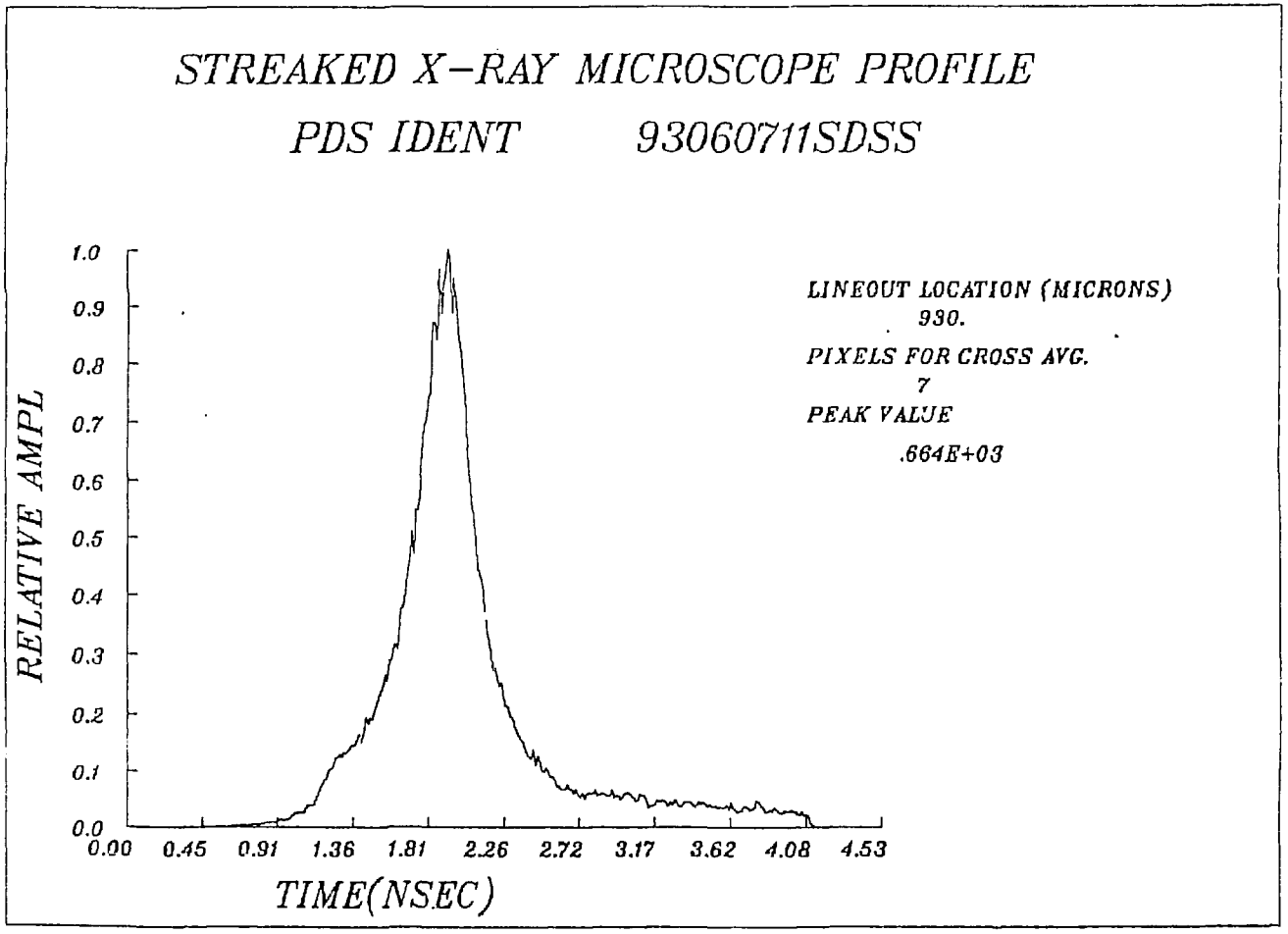
STREAKED X-RAY MICROSCOPE PROFILE
PDS IDENT 93060711SDSS
RELATIVE AMPL
1.0
0.9
0.8
0.7
0.6
0.5
0.4
0.3
0.2
0.1
0.0
0.00 0.45 0.91 1.36 1.81 2.26 2.72 3.17 3.62 4.08 4.53
TIME(NSEC)
LINEOUT LOCATION (MICRONS)
930.
PIXELS FOR CROSS AVG.
7
PEAK VALUE
.664E+03

U 09/09/83
11:13:08
Z65 KGT

Fig 2.6

DANTE-A OSCILLOSCOPE DATA
NOVETTE

SHOT 93060711

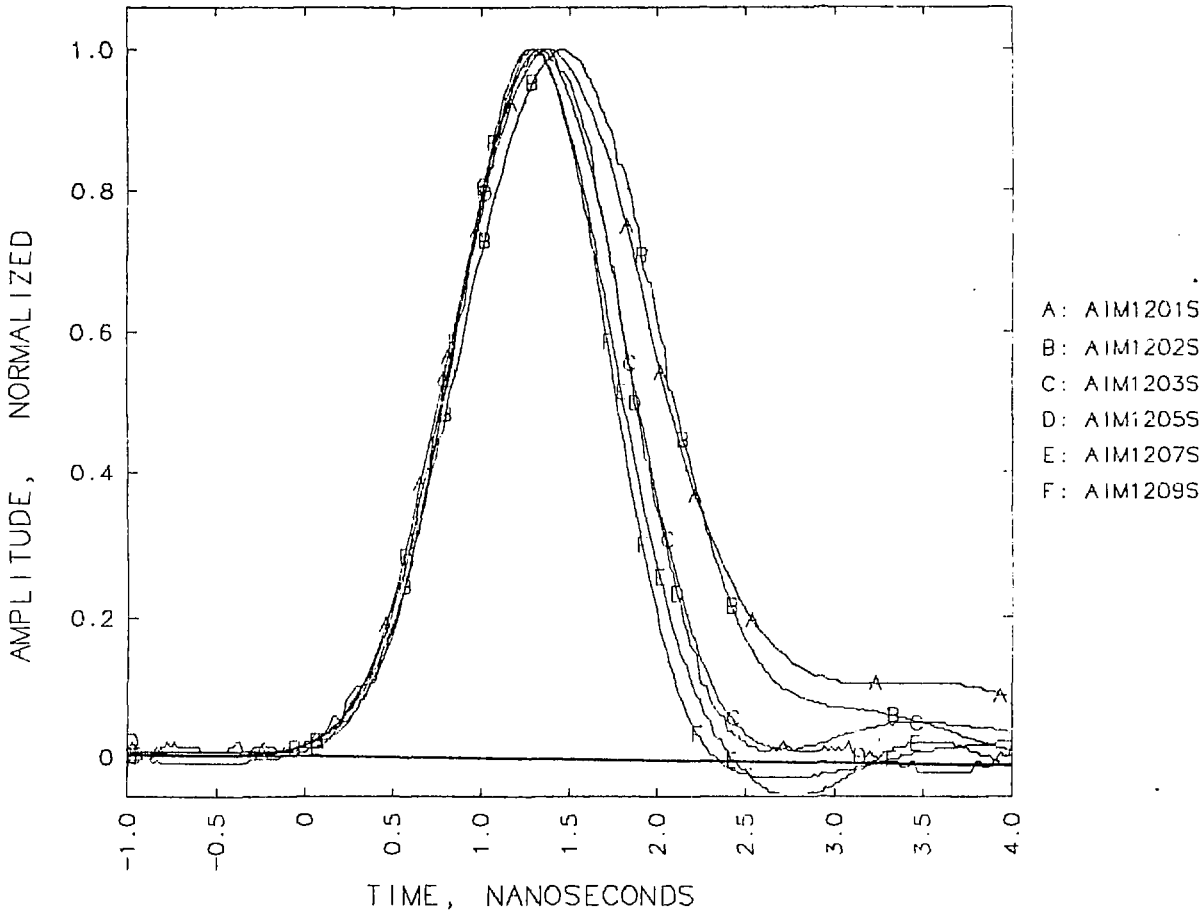

LPE

Fig 27

DANTE A NOVETTE 2WO THETA,PHI = 105,90 6/07/83 93060711 = IM12
GOLD DISK N BEAM 0 DEG ROT. .65KJ 3.98E14 W/CM2 475UM SPOT PK*FWH

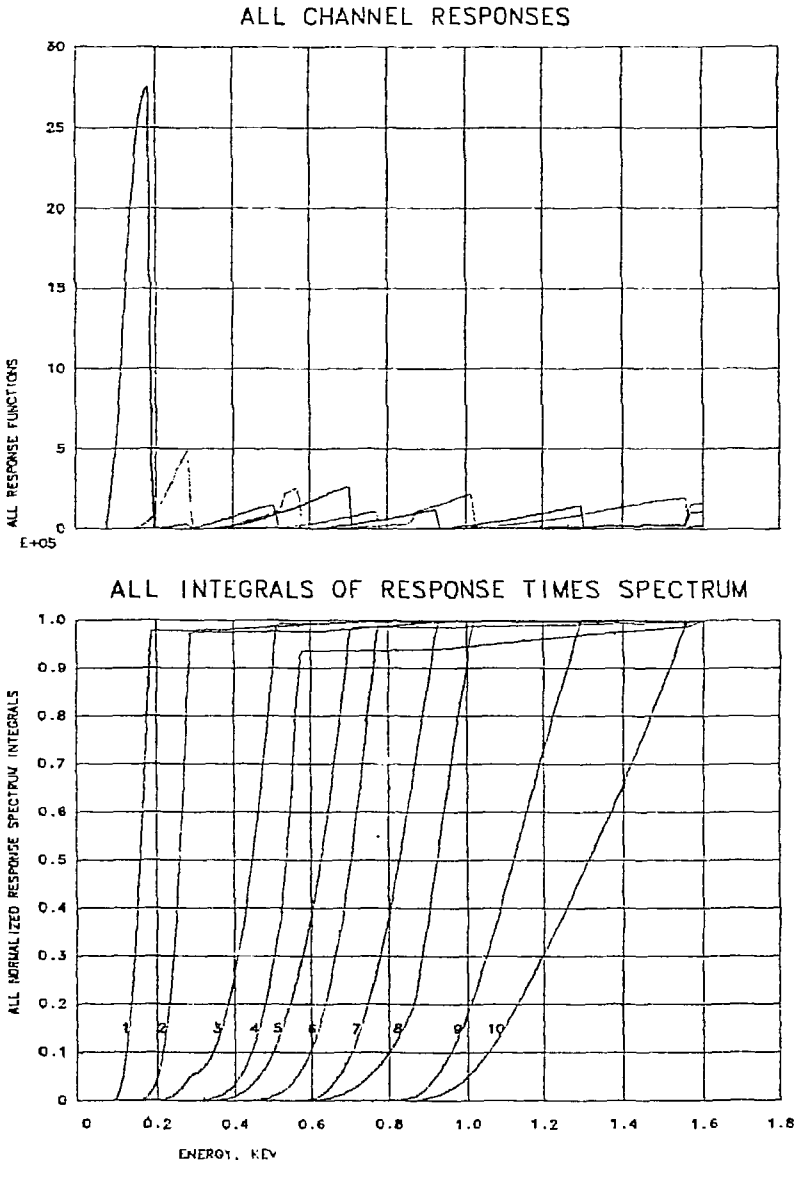

Fig 28

—— DA1M12C
O DA1M12P

R 09/09/83
08:29 40

NOVETTE 2WO LOW ENERGY XRAY SPECTRA-- GOLD DISK TARGETS

DANTE A SHOT 93060711